Article

Application of the Generalized Normal Distribution Optimization Algorithm to the Optimal Selection of Conductors in Three-Phase Asymmetric Distribution Networks

Julián Alejandro Vega-Forero [1] , Jairo Stiven Ramos-Castellanos [1] and Oscar Danilo Montoya [1,2,*]

[1] Grupo de Compatibilidad e Interferencia Electromagnética, Facultad de Ingeniería, Universidad Distrital Francisco José de Caldas, Bogotá 110231, Colombia
[2] Laboratorio Inteligente de Energía, Facultad de Ingeniería, Universidad Tecnológica de Bolívar, Cartagena 131001, Colombia
* Correspondence: odmontoyag@udistrital.edu.co

Abstract: This article addresses the problem of the optimal selection of conductors in asymmetric three-phase distribution networks from a combinatorial optimization perspective, where the problem is represented by a mixed-integer nonlinear programming (MINLP) model that is solved using a master-slave (MS) optimization strategy. In the master stage, an optimization model known as the generalized normal distribution optimization (GNDO) algorithm is proposed with an improvement stage based on the vortex search algorithm (VSA). Both algorithms work with discrete-continuous coding that allows us to represent the locations and gauges of the different conductors in the electrical distribution system. For the slave stage, the backward/forward sweep (BFS) algorithm is adopted. The numerical results obtained in the IEEE 8- and 27-bus systems demonstrate the applicability, efficiency, and robustness of this optimization methodology, which, in comparison with current methodologies such as the Newton metaheuristic algorithm, shows significant improvements in the values of the objective function regarding the balanced demand scenario for the 8- and 27-bus test systems (i.e., 10.30% and 1.40% respectively). On the other hand, for the unbalanced demand scenario, a reduction of 1.43% was obtained in the 27-bus system, whereas no improvement was obtained in the 8-bus grid. An additional simulation scenario associated with the three-phase version of the IEEE33-bus grid under unbalanced operating conditions is analyzed considering three possible load profiles. The first load profile corresponds to the yearly operation under the peak load conduction, the second case is associated with a daily demand profile, and the third operation case discretizes the demand profile in three periods with lengths of 1000 h, 6760 h, and 1000 h with demands of 100%, 60% and 30% of the peak load case. Numerical results show the strong influence of the expected demand behavior on the plan's total costs, with variations upper than USD/year 260,000.00 between different cases of analysis. All implementations were developed in the MATLAB® programming environment.

Keywords: combinatorial optimization; distribution systems; conductor selection; energy losses; power flow

1. Introduction

The network operator of the Local Distribution System depends fundamentally on the physical assets of the National Interconnected System to be able to transport electrical energy from the generation plants to the final consumer, with the distribution networks being the greatest asset that the power system represents [1]. The constant growth of societies brings with it the need to expand and repower networks. In addition, the high energy demand, the use of new technologies and the transition to e-mobility systems are factors that accelerate the thermal limits being reached in conductors [2]. All of the above entails new challenges for the network operator, who seeks to ensure the quality, reliability and safety in the provision of public service, developing an adequate and efficient planning

of its emerging electric power systems [1]. Solving problems associated with the loadability in transmission lines has marked the trend in smart electrical systems, and factors such as environmental awareness have led to the promotion of new plans for the effective and efficient expansion of distribution networks [2,3].

However, there is a risk implied in the improper selection of conductors for the electrical distribution networks, which can compromise the correct operation of the network if the conductors selected do not meet the electricity demand of all the users, making the system unreliable and inefficient, or by oversizing them which would be detrimental to the investment in addition to being an unnecessary expense of material [4]. Properly planning the electrical system better secures its good health in economic and technical terms; since energy loss is minimized, voltage profiles are optimized, and reliability and quality in service provision are improved [3]. In this sense, applying new methods that will guide the appropriate planning and expansion of electrical distribution networks will not only ensure that the system is operating correctly but will also reduce the costs associated with its implementation and development [5]. An efficient network distribution expansion plan must ensure the economic viability of the distribution company in compliance with the quality standards required by the regulatory entities [3]. The optimal conductor selection problem is a classic subproblem in the efficient expansion of the electrical distribution system [6] and can be approached through different optimization methodologies, among which heuristic algorithms and exact methods stand out. In this way, carrying out arbitrary expansions in the electrical system can lead to the detriment of the general economy of the system, which is why an adequate management and design is necessary. Thus, based on mixed-integer programming and heuristic algorithms, an efficient tool can be obtained which allows solving these types of problems [7–9], reducing costs thanks to their ability to analyze the solution space and correctly assign the elements to be installed in the electrical distribution system [10]. Linear and nonlinear approximations also allow for an adequate formulation of this type of problem since these models are solved through exact techniques available in commercial optimization packages. Implementing heuristic algorithms allows evaluating the solution space with the objective of maximizing the savings associated with investment and operating costs [11,12]. This does not involve enormous computational efforts and contributes greatly to the development of electrical networks. By improving efficiency in this type of project, investment is encouraged, bringing with it more job opportunities, greater development and technology in this sector, in addition to being able to make this type of business a market opportunity.

The following in this document is organized as follows: Section 2 presents the literature review and contributions of this. Section 3 presents the general mathematical formulation for the problem of optimal selection of conductors in asymmetric three-phase distribution networks. Section 4 presents the methodology proposed in the master stage based on the GNDO metaheuristic algorithm with an improvement stage based on hybridizing the discrete version of the vortex search algorithm (VSA) that is integrated with the slave stage based on the three-phase matricial iterative sweep power flow method. Section 5 presents information on all the test systems used, as well as the different simulation cases. Section 6 presents the information related to the computational validation of the proposed method. Section 7 presents all the numerical results of the proposed GNDO method in the test systems presented. Section 8 presents the conclusions obtained from the work presented and proposes future studies.

2. Literature Review and Contributions

Some studies, reported in the scientific literature, consider the objective function economically in the problem of optimal selection of conductors in asymmetric three-phase distribution systems. For example, in 1982 the authors of [13] developed a procedure for grading the cross section of conductors in radial distribution feeders and minimizing costs. They represented the problem using multistage dynamic programming, formulating models to represent the costs associated with the feeder, energy losses and voltage reg-

ulation as a function of conductor cross section. For the planning of optimal expansion of medium voltage power grids in [5] they proposed the improved Tabu Search/Particle Swarm algorithm (TS/IPSO), being a hybrid algorithm that proved to have better performance compared to other algorithms (such as Simulated Annealing (SA), Tabu Search (TS), Improved Genetic Algorithm (IGA), (SA/TS) Y (TS/IGA)) in high dimensional grids. The authors of [14] proposed a heuristic method where they incorporate biologically inspired structures and operators, such as recombination, mutation and fitness-based selection, the Evolutionary Strategy (ES) proves to be successful in the 8-bus system, composed of a substation and 7 radial feeders.The authors of [15] implemented an algorithm with evolutionary approaches (GA) and iterative sweep as a method to calculate power flows, voltage magnitudes and power losses, the results demonstrated the effectiveness of the proposed approach on a 69-bus radial network. For optimal driver selection, the authors of [16] proposed to solve the problem using the Harmony Search with a Differential Operator algorithm (HSDE), whose objective function was modeled to minimize the costs associated to capital investment and energy losses. The model was implemented on 16-bus and 85-bus systems, the results show better performances compared to the metaheuristic algorithm of Population Search (HSA) and Evolutionary Programming (EP).The authors of [17] implemented the Particle Swarm optimization technique for optimal single-wire ground return (SWER) conductor selection in rural distribution networks, the method was implemented on the 13-bus IEEE system describing the real 13-bus network extracted from the Namibian SWER system, the results show the effectiveness of the algorithm in terms of cost effectiveness compared to the base case, reducing the active power losses by 90.12% and improving the network voltage profiles. In 2016, the authors of [18] used the discrete particle swarm optimization algorithm (DPSO), minimizing the energy benefit cost, reducing energy losses and minimizing depreciation. This algorithm was implemented on a 26-bus and 32-bus system, with five different conductors types, the results showed that the algorithm is feasible and efficient as it improves the performance compared to the GA. The authors of [19] proposed a modified differential evolution (MDE) algorithm for conductor selection and implemented a direct approximation load flow. The objective function takes into account capital investment, active power loss and that classical technical constraints are satisfied, they considered variables such as load growth. The method was implemented on a 32-bus system, the results of which reduce the active power losses by 60% with respect to the base case by improving the voltage profiles.The authors of [20] proposed the metaheuristic crow search algorithm (CSA), taking into account the objective function and classical technical constraints. The above is implemented in a 16-bus and 85-bus system, and the results obtained show significant reductions in energy losses compared to the original network of 33.32% and 19.563%, respectively. The authors of [21] implemented the sine-cosine optimization algorithm (SCA) in the networks of the Egyptian distribution system for the optimal selection of conductors, considering the annual growth rate of the load over a period of ten years and maintaining the voltage and ampacity constraints, using a catalog of twenty conductors. Their results are satisfactory in terms of the result and the computational processing time.The authors of [22] implemented the metaheuristic salp swarm optimization algorithm to solve the optimal conductor selection in a real radial distribution system in Egypt, the results showed the effectiveness of the algorithm in satisfying the objective function and constraints, however it highlights the importance of considering feeder reinforcement to improve system hosting capacity (HC) levels, giving the possibility to connect distributed generator (DG) units.The authors of [23] implemented the Bifurcation Minimization Technique (BWMT) for optimal conductors selection, it is highlighted that the method takes into account the environmental effects on the branches resistance in addition to the load sensitivity to weathering in a 16-bus system, thus allowing a more accurate calculation of power losses in the system, the results are shown to be satisfactory when compared with the original network.The authors of [24] implemented the Whale Optimization Algorithm (WOA) to solve the optimal radial distribution network conductor selection problem, where techno-economic aspects such

as high annual load growth and payback period were considered. The objective function minimizes the cost associated with the investment and energy losses, taking into account the basic constraints, the model is implemented in a system of 16 and 85 buses obtaining favorable results compared to literature results, maximizing the overall savings and maintaining the constraints for a period of five years.The authors of [25] did simulations where customer losses were evaluated before and after implementing the model, whose objective is to achieve the best selection of conductors for the distribution system, implementing the optimization technique based on the Teaching-Learning algorithm in a 16-bus system, simulating heavy load during the Indian agricultural season; the results were satisfactory, reducing losses and improving voltage profiles.

Given the nature of the electrical power system, new methods for calculating the three-phase flow for both balanced and unbalanced loads are sought, continually improving the accuracy of proposed models, as in [26], where the authors propose the optimal selection of conductors in three-phase distribution networks through a discrete version of the meta-heuristic vortex search method using two systems structured with 8- and 27-buses under three different maximum load scenarios for 8670 hours, three percentages of consumption and a real daily load curve.

As described in the previous review of state of the art, regardless of the technique or methodology of solution used, the main objective is to reduce, as much as possible, the costs associated with planning electrical distribution networks, keeping the technical parameters within the allowable values according to the current territorial regulation, seeking to improve the quality of service received by end users and to generate a profitable environment for the companies providing the service.

Considering the literature review presented in the previous section, this paper makes the following contribution: An improvement stage is added to the master stage of the Generalized Gaussian Normal Distribution (GNDO) based metaheuristic algorithm, which combines its evolution rules with the discrete version of the Vortex Search Algorithm (VSA) to obtain a new hybrid optimizer. The main advantage of this proposed method is that it guarantees to reach a optimal local solution with the minimum standard deviation, obtaining the convergence of the objective function in a single evaluation, which allows to have a higher performance in the computational processing times.

Table 1 summarizes the studies consulted in developing state of the art, presenting the numerical method applied, the objective function under analysis, the year of publication and the corresponding citation.

The main advantages of the proposed GNDO to deal with the problem in electrical distribution network are as follows:

i. The proposed solution methodology can be implemented for any three-phase balanced and unbalanced distribution system with radial topology regardless of the load connections or the number of buses.

ii. It's exploration and exploitation stages make the proposed GNDO a robust and efficient solution methodology, in which with the help vortex search algorithm could obtain an optimal solution in a single evaluation besides using shorter processing times.

iii. Implementation and adaptation of complementary software such as Microsoft Power BI® allowed us to rigorously examine both technically and economically, the analysis of the algorithm proposed.

Table 1. Summary of the methodologies used in the literature for the problem of optimal conductor selection in distribution networks.

Sol. Methodology	Objetive Function	Operation Scenario	Refs.	Year
Evolutionary strategy	Minimize network investment costs	Maximum load on 7-bus system	[14]	2006
Genetic Algorithms	Minimizing active power losses and maximizing conductor material savings	Maximum load on 13-bus system	[27]	2011
Harmony search	Minimize the sum of capital investment and energy losses	Heavy load, simulating the agricultural season in a 16 and 85-bus system.	[16]	2011
Particle swarm optimization	Minimize capital investment depreciation, energy loss costs and maximum current capacity	Maximum load for 26- and 32-bus system	[17,18]	2012 2016
Modified Differential Evolution	Minimize fixed costs associated with network investment and variable costs associated with operation.	Two scenarios projecting annual load growth	[19]	2014
Differential evolution	Savings in conductive material costs and energy losses.	Maximum load, implemented in an unbalanced three-phase system of 19 and 34 buses.	[28]	2016
Crow search algorithm	Minimize capital cost and energy losses	scenario with peak demand in 16- and 85-buses system	[20]	2017
Sine cosine algorithm	Minimizing the annual cost of energy losses and capital investment	Peak demand, projecting 10 consecutive years of load growth in a 22-buses system.	[21]	2017
Salp swarm optimizer	Minimize energy losses and investment cost of conductors	Three scenarios at 50, 100 and 150% of nominal load and different levels of distributed generation	[22]	2018
Improved tabu search algorithm	Minimize investment cost and energy loss	Maximum load on 23-, 48- and 71-buses system	[5]	2019
Heuristic search method	Driver depression cost and annual energy losses.	Maximum load on 69- and 85-buses system	[23,29]	2016 2019
Whale optimization algorithm	Minimize the cost of energy loss and investment of conductors	Peak power in 16- and 85-buses system	[24]	2019
Teaching—learning	Minimize investment and the annual cost of losses	Peak demand scenario in 16-buses system	[25]	2020
Vortex search algorithm	Minimization of conductor investment costs and network technical losses	Balanced and unbalanced load under three scenarios, at 100% of the maximum load, 50%, and 44% of the nominal load.	[26]	2021
Newton-based metaheuristic optimizer	minimize annual energy losses and investment in conductors	Balanced and unbalanced load scenarios	[30]	2022

It's important to mention that in this study's scope only covers applying a new efficient optimization technique to select conductors in three-phase asymmetric networks with radial topologies, uncertainties regarding demand behavior are not considered. However, to present the effectiveness of the proposed GNDO, a simulation scenario with three different anual demand cases was exposed. In future works derived from this study, uncertainty in demand curves can be studied since, as evidenced in Table 1, the studied problem continues to be relevant and essential for academics and distribution companies, implying that more research is required. Additionally, we present the effectiveness of the proposed GNDO in the 8-bus grid with five different combinatorial optimization methods. The best three approaches are select for comparison in the 27-bus grid. However, for the 33-bus grid, based on the results of the 27-bus grid, we only present numerical results with the proposed GNDO because no literature reports exist for the IEEE 33-bus grid in its three-phase version.

3. Mathematical Formulation

The problem of the optimal selection of conductors in balanced (single-phase representation) and unbalanced (three-phase representation) local distribution systems (LDS) can be mathematically modeled through mixed integer nonlinear programming (MINLP) [1] where the binary (or integer) variables are related to the selection of the conductor gauge in each network section. In contrast, the continuous variables are associated with the voltages, currents and powers. The product between the trigonometric functions and the voltage causes the power balance equations to have a non-convex and non-linear behavior, making this the most significant problem in the model when it comes to determining the optimal set of conductors [10]. The mathematical model that describes the optimization problem studied in this research is presented below:

3.1. Objective Function

The objective function considers an operational evaluation horizon of one year, which seeks to minimize the costs associated with the investment in the conductor sizes and the annual energy losses. In (1)–(4), the general structure of the objective function is represented.

$$C_{loss} = C_p \sum_{h \in \Omega_h} \sum_{p \in \Omega_p} \sum_{q \in \Omega_p} \sum_{i \in \Omega_b} \sum_{j \in \Omega_b} V_{h,i}^p V_{h,j}^q Y_{ij}^{pq}\left(\lambda_{ij}^c\right) \cos\left(\phi_{h,i}^p - \phi_{h,j}^q - \phi_{h,ij}^{pq}\left(\lambda_{ij}^c\right)\right)\Delta_h, \tag{1}$$

$$C_{inv} = \sum_{c \in \Omega_C} \sum_{km \in \Omega_L} C_{km}^c L_{km} \lambda_{km}^c, \tag{2}$$

$$C_{pen} = \sum_{c \in \Omega_c} \sum_{km \in \Omega_L} P \lambda_{km}^c, \tag{3}$$

$$Z = \min\left(C_{loss} + C_{inv} + C_{pen}\right), \tag{4}$$

In (1) the variable C_{loss} represents the operating costs associated with energy losses for the evaluation period, C_p refers to the average cost of energy; Δ_h is the magnitude in hours of the evaluated period, Y_{ij}^{pq} and $\Phi_{h,ij}^{pq}$ represent the magnitude and angle of the admittance formed between the buses i and j of the phases p and q respectively, these are nonlinear functions of the binary variable λ_{ij}^c, this variable defines the "c" gauges for the conductor that joins the buses i and j; for a period of time h, $V_{h,i}^p$ and $V_{h,j}^p$ are the variables that define the voltage magnitudes, while $\Phi_{h,i}^p$ and $\Phi_{h,j}^p$ define the angles of the voltages at buses i and j of phase p respectively.

In (2), C_{inv} represents the cost of the investment, according to the selected gauge of the conductors belonging to the three-phase distribution system networks, where C_{km}^c associates the cost of the "c" type conductor along a kilometer in length, the variable L_{km} refers to the network section in kilometers formed by the buses k and m; λ_{km}^c is the binary decision variable that defines the installation of the type "c" conductor in the network fragment formed by the buses k and m.

In (3), C_{pen} represents the penalty cost, where P is a fixed-integer monetary value established by the violation of the I_{max}^c according to the conductor used for each network section, as described in (8). This penalty cost P was arbitrarily determined to be one million dollars.

In (4), Z is the value of the objective function, which corresponds to the sum of energy loss costs in the period of one year (C_{loss}), costs associated with the investment of conductors (C_{inv}) and penalties (C_{pen}) derived from violating the constraints of the distribution system, such as the thermal limit in conductors.

3.2. Set of Constraints

The optimal selection of conductors in three-phase distribution networks is subject to a set of constraints associated with the balance of active and reactive power, operating limits of the conductors, voltage regulation at buses and the binary decision variables. From (5)–(12), the set of constraints mentioned above is presented.

$$P^p_{g_{i,h}} - P^p_{d_{i,h}} = \sum_{p\in\Omega_h}\sum_{q\in\Omega_p}\sum_{i\in\Omega_b}\sum_{j\in\Omega_b} V^p_{h,i}V^q_{h,j}Y^{pq}_{ij}\left(\lambda^c_{ij}\right)cos\left(\phi^p_{h,i} - \phi^q_{h,j} - \phi^{pq}_{h,ij}\left(\lambda^c_{ij}\right)\right), \begin{bmatrix}\forall i \ \in \Omega_b \\ \forall h \ \in \Omega_h \\ \forall p \ \in \Omega_p\end{bmatrix}, \quad (5)$$

$$Q^p_{g_{i,h}} - Q^p_{d_{i,h}} = \sum_{p\in\Omega_h}\sum_{q\in\Omega_p}\sum_{i\in\Omega_b}\sum_{j\in\Omega_b} V^p_{h,i}V^q_{h,j}Y^{pq}_{ij}\left(\lambda^c_{ij}\right)sen\left(\phi^p_{h,i} - \phi^q_{h,j} - \phi^{pq}_{h,ij}\left(\lambda^c_{ij}\right)\right), \begin{bmatrix}\forall i \ \in \Omega_b \\ \forall h \ \in \Omega_h \\ \forall p \ \in \Omega_p\end{bmatrix}, \quad (6)$$

$$I^p_{km,h} = f\left(V^p_{h,k}, V^p_{h,m}, \phi^p_{h,k}, \phi^p_{h,m}, \lambda^c_{km}, R^c_{km}, X^c_{km}\right), \begin{bmatrix}\forall\{km\} \ \in \Omega_L \\ \forall h \ \in \Omega_h \\ \forall p \ \in \Omega_p\end{bmatrix}, \quad (7)$$

$$\left[I^p_{km,h}\right] \le \sum_{C\in\Omega}\lambda^c_{km}I^{max}_c, \begin{bmatrix}\forall\{km\} \ \in \Omega_L \\ \forall h \ \in \Omega_h \\ \forall p \ \in \Omega_p\end{bmatrix}, \quad (8)$$

$$V^{min}_i \le V^p_{i,h} \le V^{max}_i, \begin{bmatrix}\forall i \ \in \Omega_b \\ \forall h \ \in \Omega_h \\ \forall p \ \in \Omega_p\end{bmatrix}, \quad (9)$$

$$\sum_{c\in\Omega_c}\lambda^c_{km} = 1[\forall\{km\}\in\Omega_L], \quad (10)$$

$$\sum_{km\in\Omega_L}\sum_{c\in\Omega_c}\lambda^c_{km} = n - 1, \quad (11)$$

$$\lambda^c_{km} \in \{0,1\} \ [\forall \ \{km\}\in\Omega_L, \forall c\in\Omega_c], \quad (12)$$

From the previous equations, Ω_L contains the set of network sections of the distribution system, Ω_b establishes all the buses belonging to the system, Ω_h defines the periods of load duration and the set Ω_p contains the phases of the system.

In (5) and (6), the active and reactive power balance is defined for each bus, phase and time period, where $P^p_{g_{i,h}}$ and $P^p_{d_{i,h}}$ represent active power generation and demand; similarly, $Q^p_{g_{i,h}}$ and $Q^p_{d_{i,h}}$ represent reactive power generation and demand, respectively. In (7), the current is calculated that flows in the network section formed by the buses *k* and *m*, of phase *p*, in a period of time *h*, where $I^p_{km,h}$ is a function of the magnitude of the voltages, angles, gauge of the conductor and its resistance (R^c_{km}) and reactance (X^c_{km}) parameters. The inequality constraint presented in (8) guarantees that the current flow in the network section formed by the buses *k* and *m* of the phase *p*, in a period of time *h*, does not exceed the thermal limit of the gauge selected for the network section, i.e., I^{max}_c. Constraint (9) ensures that for each bus *i* of phase *p* in a period of time *h*, the system voltage is within the regulatory range defined by the limit greater than or equal to the minimum voltage V^{min}_i and the limit less than or equal to the maximum voltage V^{max}_i. Equation (10) guarantees that for the network section formed by the buses *k* and *m*, only one "*c*" type conductor is selected; Additionally, in (11), it is guaranteed that the total number of conductors selected is equal to the number of buses in the system *n* minus 1. Finally, in (12), the discrete binary nature of the decision variable is defined with respect to the "*c*" type gauge for the section of network formed between the buses *k* and *m*.

The MINLP mathematical model defined in (1)–(12) represents the general formulation of the problem of optimal selection of conductors in three-phase systems with both balanced and unbalanced structures [30]. According to the analyzed case study, the dimension of the solution space can be as large as desired, due to its dependence on the number of network sections "*l*" and the number of candidate gauges "*c*", with c^l as solution space. This represents one of the biggest complications for this type of problem [31].

As an example of the above, considering a radial configuration of the distribution system, which is made up of 20 network sections (*l* = 20), and additionally, there are 5 candidate gauges (*c* = 5), the solution space will be 5^{20}, which is a size equivalent to 95, 367, 431, 640, 625, with approximately 95 billion possible solutions, so evaluating each of these possible solutions becomes a cumbersome and inefficient task. To face this difficulty and to obtain an optimal solution in reasonable computation times, a master-slave optimization

approach is proposed to solve the MINLP mathematical model based on the generalized normal distribution optimization algorithm GNDO and the three-phase matricial iterative sweep algorithm as a power flow method.

4. Solution Methodology

This document proposes the implementation of the metaheuristic algorithm GNDO [32] in the master stage and three-phase matricial formulation of the iterative sweep method for calculating power flow at the slave stage. The master stage will be responsible for the optimal selection of gauges for all branches using integer coding [26] and in the slave stage, each set of conductors will be evaluated to determine the value of the objective function (total costs of energy losses) for a given planning period. Similar to most metaheuristic optimization algorithms, the GNDO works with an initial population x_i^t that has the following structure (13):

$$x_i^t = [3, 5, \ldots, g, \ldots, 4],\tag{13}$$

where t is the iteration counter of the GNDO and "g" refers to a gauge available in the set of conductors. It is important to note that the dimension of the matrix associated with the initial population x_i^t is of the form $N_i \times d$, where N_i is the number of individuals in the initial population and d is the dimension of the problem corresponding to the number of lines in the distribution system. In the following subsections, the most important aspects of the master and slave stages are presented.

4.1. Slave Stage: Three-Phase Power Flow

Distribution networks have a radial or tree-like structure. It is common in the analysis of the calculation of the power flow in this type of electrical network to find methods based on graph theory, where with the help of the incidence matrix, it is possible to represent the topological structure of the distribution network relating the buses with the branches of the system; in this way, if there is a branch between two buses of a graph, both buses will be connected [32]. The matricial formulation of the iterative sweep method is an approach for calculating power flow based on graph theory, in which Kirchhoff's laws are used to calculate the currents of the system buses, starting from the terminal buses toward the slack bus (backward sweep), as well as the voltage drops in the different segments of the network, starting from the slack bus toward the terminal buses (forward sweep) [33]. This solution method is commonly known as the backward/forward sweep method.

To illustrate the structure of the incidence matrix, consider the distribution system shown in Figure 1. This radial network is made up of 4 branches and 5 buses.
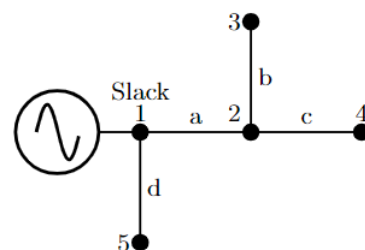

Figure 1. Single-line diagram of the proposed example.

To represent the topology of the electrical network, the relationship between the buses and the phases of the branches of the system is established by the three-phase incidence matrix Λ, where the positive direction of the branch current is defined so that it always flows out of the bus, as shown in (14).

$$\Lambda_{ix,jz} = \begin{cases} +1 & \text{if line } i \text{ is connected to bus } j \text{ and the current} \\ & \text{of phase } x \text{ leaves the bus.} \\ -1 & \text{if line } i \text{ is connected to bus } j \text{ and the current} \\ & \text{of phase } x \text{ enters the bus.} \\ 0 & \text{if phase } x \text{ of branch } i \text{ is not connected to phase} \\ & z \text{ of bus } j \end{cases} \tag{14}$$

where i corresponds to the branches of the system, x to the phases of the branches, j to the buses of the system and z to the phases of the buses; in this way, the bus connections and the three-phase incidence matrix Λ are shown in Table 2 and in (15), respectively.

$$\Lambda_{ix,jz} = \begin{bmatrix} 1 & 0 & 0 & -1 & 0 & 0 & 0 & 0 & 0 & 0 & 0 & 0 & 0 & 0 & 0 \\ 0 & 1 & 0 & 0 & -1 & 0 & 0 & 0 & 0 & 0 & 0 & 0 & 0 & 0 & 0 \\ 0 & 0 & 1 & 0 & 0 & -1 & 0 & 0 & 0 & 0 & 0 & 0 & 0 & 0 & 0 \\ 0 & 0 & 0 & 1 & 0 & 0 & -1 & 0 & 0 & 0 & 0 & 0 & 0 & 0 & 0 \\ 0 & 0 & 0 & 0 & 1 & 0 & 0 & -1 & 0 & 0 & 0 & 0 & 0 & 0 & 0 \\ 0 & 0 & 0 & 0 & 0 & 1 & 0 & 0 & -1 & 0 & 0 & 0 & 0 & 0 & 0 \\ 0 & 0 & 0 & 1 & 0 & 0 & 0 & 0 & 0 & -1 & 0 & 0 & 0 & 0 & 0 \\ 0 & 0 & 0 & 0 & 1 & 0 & 0 & 0 & 0 & 0 & -1 & 0 & 0 & 0 & 0 \\ 0 & 0 & 0 & 0 & 0 & 1 & 0 & 0 & 0 & 0 & 0 & -1 & 0 & 0 & 0 \\ 1 & 0 & 0 & 0 & 0 & 0 & 0 & 0 & 0 & 0 & 0 & 0 & -1 & 0 & 0 \\ 0 & 1 & 0 & 0 & 0 & 0 & 0 & 0 & 0 & 0 & 0 & 0 & 0 & -1 & 0 \\ 0 & 0 & 1 & 0 & 0 & 0 & 0 & 0 & 0 & 0 & 0 & 0 & 0 & 0 & -1 \end{bmatrix} \tag{15}$$

Table 2. Bus connections for the example shown in Figure 1.

Nomenclature of Branch i	From Bus j	To Bus k
a	1	2
b	2	3
c	2	4
d	1	5

This three-phase incidence matrix is divided into two submatrices, which are related with respect to generation (this is possible because the slack bus is located on bus 1) and demand, as shown in (16).

$$\Lambda_{ix,jz} \leftrightarrow \Lambda_{3\phi} = \begin{bmatrix} \Lambda_{s3\phi} & \Lambda_{d3\phi} \end{bmatrix}, \tag{16}$$

where $\Lambda_{s3\Phi}$ corresponds to the first three columns of $\Lambda_{3\Phi}$ (slack bus) and $\Lambda_{d3\Phi}$ corresponds to the rest of the columns of $\Lambda_{3\Phi}$ (demand buses).

Now, we proceed to define the voltage drops per phase for each of the branches of the system. These voltage drops are defined as the difference between the node voltages per phase that connect each of the branches; in this way, we get:

$$\mathbb{E}_{r3\phi} = \Lambda_{s3\phi} \, V_{s3\phi} + \Lambda_{d3\phi} V_{d3\phi}, \tag{17}$$

where $\mathbb{E}_{r3\Phi}$ is a matrix that includes all voltage drops, in which $V_{s3\Phi} = V_{\{1-3\}3\Phi}$ and $V_{d3\Phi}$ is a matrix that includes all the voltages in the demand buses. On the other hand, it is possible to define the bus currents ($I_{n3\Phi}$) as

$$I_{n3\phi} = \begin{bmatrix} I_{s3\phi} & I_{d3\phi} \end{bmatrix}^T, \tag{18}$$

where $I_{s3\Phi}$ and $I_{d3\Phi}$ are the generation and demand currents per phase, respectively. In the same way, the generation and demand currents can be deduced as shown below:

$$I_{s3\phi} = \Lambda_{s3\phi}^T \mathbb{J}_{r3\phi}, \tag{19}$$

$$I_{d3\phi} = \Lambda_{d3\phi}^T \mathbb{J}_{r3\phi}, \tag{20}$$

In contrast, the voltage drops per phase in each of the branches can be defined through the three-phase impedance matrix for distribution lines, which contains information of each three-phase line impedance and the currents flowing around each one of the branches, as expressed in matrix form in (21).

$$
\begin{bmatrix}
\mathbb{E}_{aA} \\
\mathbb{E}_{aB} \\
\mathbb{E}_{aC} \\
\mathbb{E}_{bA} \\
\mathbb{E}_{bB} \\
\mathbb{E}_{bC} \\
\mathbb{E}_{cA} \\
\mathbb{E}_{cB} \\
\mathbb{E}_{cC} \\
\mathbb{E}_{dA} \\
\mathbb{E}_{dB} \\
\mathbb{E}_{dC}
\end{bmatrix}
=
\begin{bmatrix}
Z_{aAA} & Z_{aAB} & Z_{aAC} & 0 & 0 & 0 & 0 & 0 & 0 & 0 & 0 & 0 \\
Z_{aBA} & Z_{aBB} & Z_{aBC} & 0 & 0 & 0 & 0 & 0 & 0 & 0 & 0 & 0 \\
Z_{aCA} & Z_{aCB} & Z_{aCC} & 0 & 0 & 0 & 0 & 0 & 0 & 0 & 0 & 0 \\
0 & 0 & 0 & Z_{bAA} & Z_{bAB} & Z_{bAC} & 0 & 0 & 0 & 0 & 0 & 0 \\
0 & 0 & 0 & Z_{bBA} & Z_{bBB} & Z_{bBC} & 0 & 0 & 0 & 0 & 0 & 0 \\
0 & 0 & 0 & Z_{bCA} & Z_{bCB} & Z_{bCC} & 0 & 0 & 0 & 0 & 0 & 0 \\
0 & 0 & 0 & 0 & 0 & 0 & Z_{cAA} & Z_{cAB} & Z_{cAC} & 0 & 0 & 0 \\
0 & 0 & 0 & 0 & 0 & 0 & Z_{cBA} & Z_{cBB} & Z_{cBC} & 0 & 0 & 0 \\
0 & 0 & 0 & 0 & 0 & 0 & Z_{cCA} & Z_{cCB} & Z_{cCC} & 0 & 0 & 0 \\
0 & 0 & 0 & 0 & 0 & 0 & 0 & 0 & 0 & Z_{dAA} & Z_{dAB} & Z_{dAC} \\
0 & 0 & 0 & 0 & 0 & 0 & 0 & 0 & 0 & Z_{dBA} & Z_{dBB} & Z_{dBC} \\
0 & 0 & 0 & 0 & 0 & 0 & 0 & 0 & 0 & Z_{dCA} & Z_{dCB} & Z_{dCC}
\end{bmatrix}
\begin{bmatrix}
\mathbb{J}_{aA} \\
\mathbb{J}_{aB} \\
\mathbb{J}_{aC} \\
\mathbb{J}_{bA} \\
\mathbb{J}_{bB} \\
\mathbb{J}_{bC} \\
\mathbb{J}_{cA} \\
\mathbb{J}_{cB} \\
\mathbb{J}_{cC} \\
\mathbb{J}_{dA} \\
\mathbb{J}_{dB} \\
\mathbb{J}_{dC}
\end{bmatrix}
\tag{21}
$$

From (21) the following can be obtained:

$$
\mathbb{E}_{r3\phi} = Z_{r3\phi}\mathbb{J}_{r3\phi} \, ,
\tag{22}
$$

Thus, from (22) $\mathbb{J}_{r3\Phi}$ can be found and replaced in (20) as follows:

$$
I_{d3\phi} = \Lambda_{d3\phi}^{T} Z_{r3\phi}^{-1}\mathbb{E}_{r3\phi},
\tag{23}
$$

Replacing (16) in (23) obtains:

$$
I_{d3\phi} = \Lambda_{d3\phi}^{T} Z_{r3\phi}^{-1}(\Lambda_{s3\phi}\, V_{s3\phi} + \Lambda_{d3\phi} V_{d3\phi}) \, ,
\tag{24}
$$

$$
I_{d3\phi} = \Lambda_{d3\phi}^{T} Z_{r3\phi}^{-1}\Lambda_{s3\phi}\, V_{s3\phi} + \Lambda_{d3\phi}^{T} Z_{r3\phi}^{-1}\Lambda_{d3\phi} V_{d3\phi} \, ,
\tag{25}
$$

Taking into account that:

$$
Y_{dg3\phi} = \Lambda_{d3\phi}^{T} Z_{r3\phi}^{-1}\Lambda_{s3\phi},
\tag{26}
$$

$$
Y_{dd3\phi} = \Lambda_{d3\phi}^{T} Z_{r3\phi}^{-1}\Lambda_{d3\phi} \, ,
\tag{27}
$$

Equations (26) and (27) can be replaced in (25)

$$
I_{d3\phi} = Y_{dg3\phi}V_{s3\phi} + Y_{dd3\phi}\, V_{d3\phi},
\tag{28}
$$

The main objective is to find a function of the form $V_{d3\Phi} = f(I_{d3\Phi})$ in which the three-phase demand voltages are related to the three-phase demand currents, clearing $V_{d3\Phi}$ from (28), the expression (29) is obtained

$$
\mathrm{V}_{d3\phi} = -Y_{dd3\phi}^{-1}(I_{d3\phi} + Y_{dg3\phi}V_{s3\phi})
\tag{29}
$$

However, in (29) $I_{d3\Phi}$ is still an unknown variable. This three-phase demand current will depend on the type of load that will be connected, i.e., Star connection (Y) or in Delta (Δ). Therefore, in the case in which the loads that are connected to the electrical system have a star connection, we get (30)–(32).

$$
I_{kA} = \left(\frac{S_{kA}}{V_{kA}}\right)^{*},
\tag{30}
$$

$$
I_{kB} = \left(\frac{S_{kB}}{V_{kB}}\right)^{*},
\tag{31}
$$

$$
I_{kc} = \left(\frac{S_{kC}}{V_{kC}}\right)^{*},
\tag{32}
$$

On the other hand, in the case that the connection of the loads is given by Delta connections, we obtain (33)–(35).

$$I_{kA} = \left(\frac{S_{kA}}{V_{kA} - V_{kB}} \right)^* - \left(\frac{S_{kC}}{V_{kC} - V_{kA}} \right)^*, \tag{33}$$

$$I_{kB} = \left(\frac{S_{kB}}{V_{kB} - V_{kC}} \right)^* - \left(\frac{S_{kA}}{V_{kA} - V_{kB}} \right)^*, \tag{34}$$

$$I_{kC} = \left(\frac{S_{kC}}{V_{kC} - V_{kA}} \right)^* - \left(\frac{S_{kB}}{V_{kB} - V_{kC}} \right)^*, \tag{35}$$

for $\forall k \in \Omega_b$ where k refers to the bus number. Thus, rewriting Equation (29) in terms of the following iteration, we get (36).

$$V_{d3\phi}^{t+1} = -Y_{dd3\phi}^{-1}(I_{d3\phi} + Y_{dg3\phi}V_{s3\phi}), \tag{36}$$

where t is the iteration counter. It is common for the power flow analysis to handle a representation per unit of all the electrical variables, which implies that the voltage of the substation can be defined with a positive sequence, as shown below: $V_{s3\Phi} = \begin{bmatrix} 1\angle 0, & 1\angle -120, & 1\angle 120 \end{bmatrix}^T$. In the same way, for expression (36) to be valid, it must meet the expression defined in (37).

$$\left| V_{d3\phi}^{t+1} - V_{d3\phi}^{t} \right| \leq \epsilon, \tag{37}$$

where ϵ is the maximum acceptable error value, with a recommended value of 1×10^{-10}. To determine the three-phase power losses, expression (38) is used, which describes the Joule effect.

$$Ploss_{3\phi} = \mathbb{R}e(sum(\mathbb{E}_{r3\phi}^{t+1})^T(\mathbb{J}_{3\phi}^{t+1})^*), \tag{38}$$

Finally, to represent the matricial reformulation of the three-phase iterative sweep, the flow diagram is presented in Figure 2.

Observation 1. Once the power losses are found for the proposed time period h, with the help of Equation (38), the value of the objective function associated with the costs of energy losses expressed in (1) is obtained, which can be found according to the following expression:

$$C_{loss} = C_p Ploss_{3\phi} \Delta_h, \tag{39}$$

4.2. Master Stage: GNDO Metaheuristic Algorithm

The GNDO is a metaheuristic method also known as generalized normal distribution optimization, which is based on the Gaussian distribution model, where each individual makes use of this curve to improve their position. The most important characteristic of the GNDO is that it does not need any type of special control parameter, but on the contrary, it only requires the initial population and assigning the terminal condition before running the algorithm. The general model of Gaussian distribution is represented in (40), where x is a random variable that corresponds to the distribution probability, which has a location parameter μ and scale parameter δ [32].

$$f(x) = \frac{1}{\sqrt{2\pi}\delta} exp\left(\frac{(x - \mu)^2}{2\delta^2} \right), \tag{40}$$

According to (39), the most important variables in the normal distribution are the location parameter (μ) and the scale parameter (δ), both used to express the mean value and standard variance of random variables, respectively [32].

Start: Three-phase BFS power flow

Enter the parameters and characteristics of the test systems

Build the incidence matrix of the form

$$\Lambda_{3\phi} = \begin{bmatrix} \Lambda_{s3\phi} & \Lambda_{d3\phi} \end{bmatrix}$$

Build the impedence matrix $Z_{3\phi}$

Initialize the phase voltages

$$V_{s3\phi} = \begin{bmatrix} 1\angle 0 \\ 1\angle 120 \\ 1\angle 240 \end{bmatrix}$$

Calculate $I^t_{d3\phi}$ according to the load connection, i.e, Y or Δ

Yields $V^{t+1}_{d3\phi} = -Y^{-1}_{dd3\phi}(I_{d3\phi} + Y_{dg3\phi}V_{s3\phi})$

Assign $V^t_{d3\phi} = V^{t+1}_{d3\phi}$

Meets $|V^{t+1}_{d3\phi} - V^t_{d3\phi}| \le \epsilon$

NO

Increase the iterative counter t by 1

YES

Calculate $Ploss_{3\phi} = \mathbb{R}(sum(\mathbb{E}^{t+1}_{r3\phi})^T(\mathbb{J}^{t+1}_{r3\phi}))$
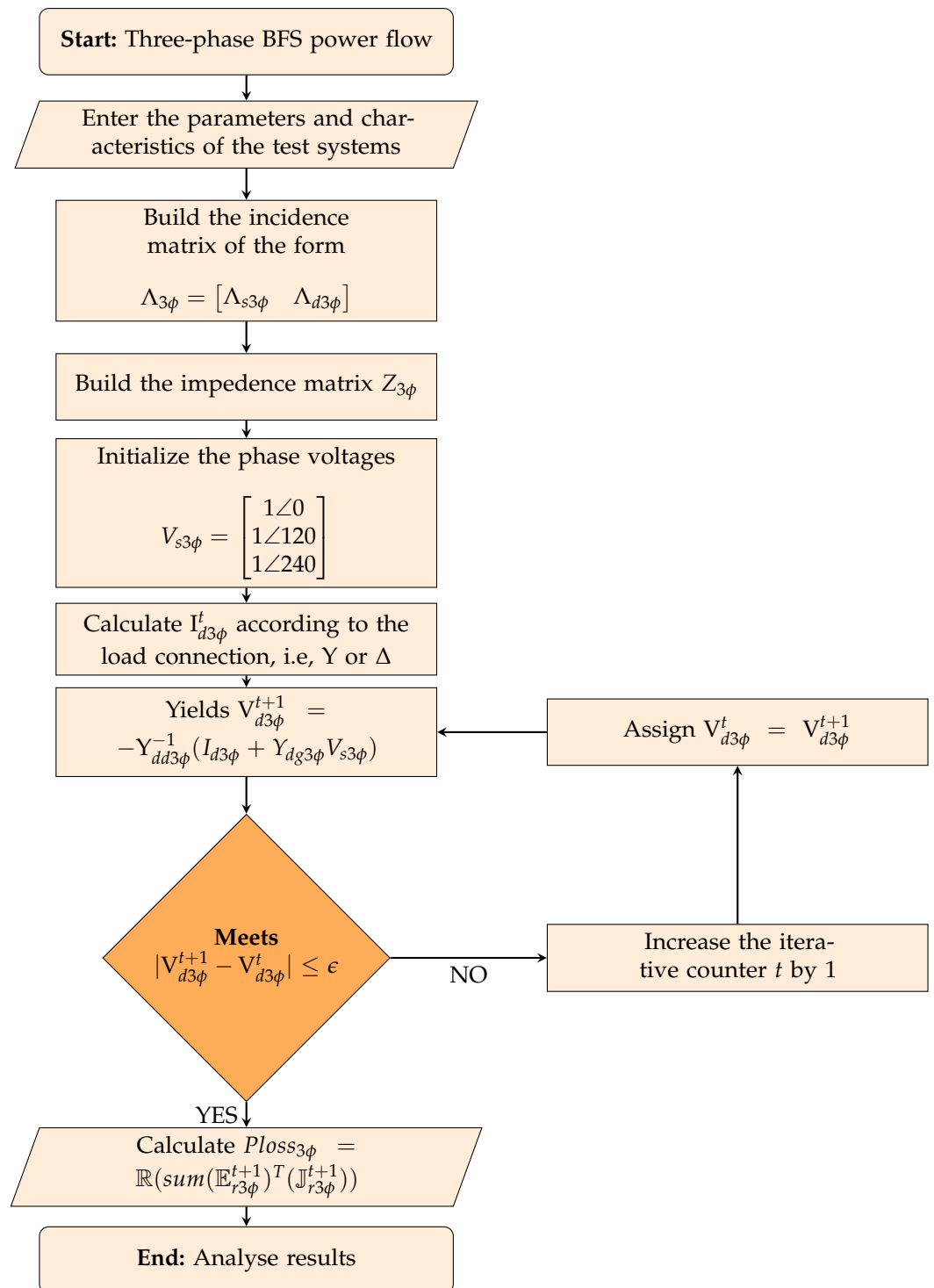
End: Analyse results

Figure 2. Flowchart used for the BFS method.

4.2.1. Local Exploitation

In this stage of exploitation, a broad search is carried out to find the best solution found thus far to verify whether there are better solutions in an attempt to accelerate the speed of convergence [34]. The process of local exploitation involves finding better optimal solutions around the current positions of all the individuals in the solution [32]. Therefore, taking as a reference the relationship between all the individuals of the solution in the current population and the normal distribution, in addition to seeking to accelerate the speed of convergence, we seek to maintain the quality of the solutions found [34], thus obtaining the following model:

$$v_i^t = \mu_i + \delta_i \eta, \quad i = 1, 2, ..., N_{i\cdot}. \tag{41}$$

In (41), i represents the *ith* individual solution, n corresponds to a penalty factor, δ_i represents the generalized standard variation, μ_i represents the generalized mean position, and v_i^t corresponds to a vector of the current solution, it is important to note that N_i corresponds to the total number of individuals in the population. The terms μ_i, δ_i and η can be obtained as follows:

$$\mu_i = \frac{1}{3}\left(x_i^t + x_{best}^t + M\right), \tag{42}$$

$$\delta_i = \frac{1}{\sqrt{3}}\left((x_i^t - \mu_i)^2 + (x_{best}^t - \mu_i)^2 + (M - \mu_i)^2\right)^{\frac{1}{2}}, \tag{43}$$

$$\eta = \begin{cases} (-\log(\lambda_1))^{\frac{1}{2}} \cos(2\pi\lambda_2), & if \ a \leq b \\ (-\log(\lambda_1))^{\frac{1}{2}} \cos(2\pi\lambda_2 + \pi), & if \ a > b \end{cases}, \tag{44}$$

where λ_1, λ_2, a and b correspond to random numbers between 0 and 1, with a uniform distribution; x_{best}^t corresponds to a vector containing the best solution found so far; and M represents a vector containing the average position of the current individuals of the population t, as defined in (45).

$$M = \frac{1}{N_i} \sum_{i=1}^{N_i} x_i^t, \tag{45}$$

4.2.2. Global Exploration

The purpose of this exploration stage is to determine and locate promising new regions of the large solution space [32]. This is because μ_i may end up being a local minimum, as the case may be, so performing the search around this parameter may not be sufficient to improve the quality of the solutions. In this way, exploring the search space as much as possible will avoid being trapped in local minima [34]. The global exploration in the GNDO can be defined as follows:

$$v_i^t = x_i^t + \beta * (|\lambda_3|. * v_1) + (1 - \beta) * (|\lambda_4|. * v_2), \tag{46}$$

where λ_3 and λ_4 are two random numbers subject to the standard normal distribution, β represents the adjustment parameter, which is randomly selected between 0 and 1, and both v_1 and v_2 are two vectors defined as observed in (47) and (48).

$$v_1 = \begin{cases} x_i^t - x_j^t, & if \ A_f(x_i^t) < A_f(x_j^t) \\ x_j^t - x_i^t, & Otherwise \end{cases}, \tag{47}$$

$$v_2 = \begin{cases} x_k^t - x_m^t, & if \ A_f(x_k^t) < A_f(x_m^t) \\ x_m^t - x_k^t, & Otherwise \end{cases}, \tag{48}$$

In (47) and (48), j, k, and m are three random integers, whose values range between 1 and the total number of individuals in the population. It is important to verify that these values are different from each other, as well as from the current individual i for iteration t.

On the other hand, $A_f(x_{i,j,k,m}^t)$ represents the value of the objective function for the vectors i, j, ks and m of the current population t. To ensure the viability of each generation in the solution space, (49) is used.

$$
v_{i,l}^t = \begin{cases} v_{i,l}^t, & if\ x_l^{min} \leq v_{i,l}^t \leq x_l^{max} \\ x_{best,l}^t, & Otherwise \end{cases}, \tag{49}
$$

where x_l^{min} and x_l^{max} are the integer values corresponding to the minimum and maximum values of the set of conductors available for installation in the distribution grid under study, which are evaluated from the first position to position d of the vector $v_{i,l}^t$ with the help of the decision variable l. It is important to clarify that d represents the dimension of the problem studied. $v_{i,l}^t$ represents the gauge value of the ith individual solution for a given position in the vector according to the decision variable l. On the other hand, $x_{best,l}^t$ refers to the value of the decision variable l for the best current solution found so far.

To maintain the best solution within the next generation of the population, the following expression is used:

$$
x_i^{t+1} = \begin{cases} v_i^t, & if\ A_f(v_i^t) \leq A_f(x_i^t) \\ x_i^t, & Otherwise \end{cases}, \tag{50}
$$

4.3. Improvement of the Exploration and Exploitation of the Solution Space

In order to obtain better results in the exploration and exploitation of the solution space, a modified version of the GNDO base algorithm with the vortex search algorithm is proposed [26]. The vortex search algorithm (VSA) is inspired by the vortex pattern created by the vortex flow of agitated fluids, making it a fairly simple algorithm in addition to being computationally efficient, so it is a good candidate for the solution of real-life optimization problems [35]. The VSA works with continuous variables [33]. Therefore, a discrete version will be used to determine the correct assignment of gauges to be installed in the branches of the different distribution systems. Thus, the initial center of the hyper-ellipse is defined in (51).

$$
\mu_0 = \frac{x^{min} + x^{max}}{2}, \tag{51}
$$

where $x^{min} \in N^{dx1}$ and $x^{max} \in N^{dx1}$ are vectors that contain integers and have a size determined by the dimension of the solution space d ($d = n-1$), where n is the number of buses. It is important to clarify that μ_0 must be rounded up to the nearest integer value. On the other hand, the generation of candidate solutions is obtained with the help of the Gaussian normal distribution as seen in (52).

$$
v_i^t = p\left(\varsigma_i^t, \mu_t, \Sigma\right) = \frac{1}{\sqrt{2\pi^d |\Sigma|}} exp\left\{ -\frac{1}{2}\left(\varsigma_i^t - \mu_t\right)^\tau \Sigma^{-1}\left(\varsigma_i^t - \mu_t\right) \right\}, \tag{52}
$$

where $\zeta_i^t \in \mathbb{R}^{dx1}$ is a vector with dimension d full of random values, $\mu_t \in \mathbb{R}^{dx1}$ which represents the center of the hyper-ellipse for each iteration t, and $\sum \in \mathbb{R}^{dx1}$ is the covariance matrix. This covariance matrix is worked as shown in [26], where it is described as a matrix that has identical values in its diagonal and null values outside it, as (53) shows.

$$
\Sigma = \sigma_0 \mathbb{I}, \tag{53}
$$

where σ_0 is the variance of the Gaussian distribution and $\mathbb{I}$ is the identity matrix with the appropriate dimensions. In the same way, the value σ_0 is found as follows:

$$
\sigma_0 = \frac{\max\{x^{max}\} - \min\{x^{min}\}}{2}, \tag{54}
$$

Here, σ_0 can be considered the initial radius (i.e., r_0). Because an adequate exploration of the solution space is required in the initial phases. r_0 is chosen to be a large value [36] (note that $\max\{x^{\max}\}$ obtains the maximum value of the vector $x^{\max}$ and $\max\{x^{\min}\}$ obtains the minimum value $x^{\max}$, respectively). The use the incomplete gamma function (see [33]) allows finding the optimal solution during the search process the optimal solution can be found. This, because the radius progressively decreases until it reaches zero, which can be seen in (55).

$$\mathrm{Y}(x, a) = \int_0^x e^{-t} t^{a-1} dt, \tag{55}$$

In (55), a is a shape parameter greater than zero, and x is a random parameter greater than or equal to zero. Thus, in order to determine the adaptive size of the radius for each iteration, the incomplete gamma function is used, as presented in [33] and (56)

$$r_t = \sigma_0 \mathrm{Y}^{-1}(x, a_t), \tag{56}$$

where a_t is a parameter obtained as shown in (57)

$$a_t = \frac{t_{max} - t}{t_{max}}, \tag{57}$$

where t_{max} corresponds to the total number of iterations ($t_{max} = 1000$); in the same way as in (55), the parameter x is selected as 0.1, as reported in [33]. To advance the process of the exploration and exploitation search, it is necessary to update the new center of the hyper-ellipse (μ_{t+1}), which will be selected as the best individual solution contained in v_i^t, where the minimum value of the objective function will be presented, which in turn is known as x_{best}^t.

It is important to mention that there is the possibility of having a candidate solution outside the limits established by the solution space, so it is necessary and essential to review the values of the minimum and maximum limits, as shown in (49).

Finally, to represent the general improved implementation of the GNDO based on ellipses of variable radius, the flow diagrama is presented in Figure 3.

Improved Implementation of the GNDO Based on Ellipses of Variable Radius

The improved implementation of the GNDO based on ellipses of variable radius is presented in Algorithm 1.
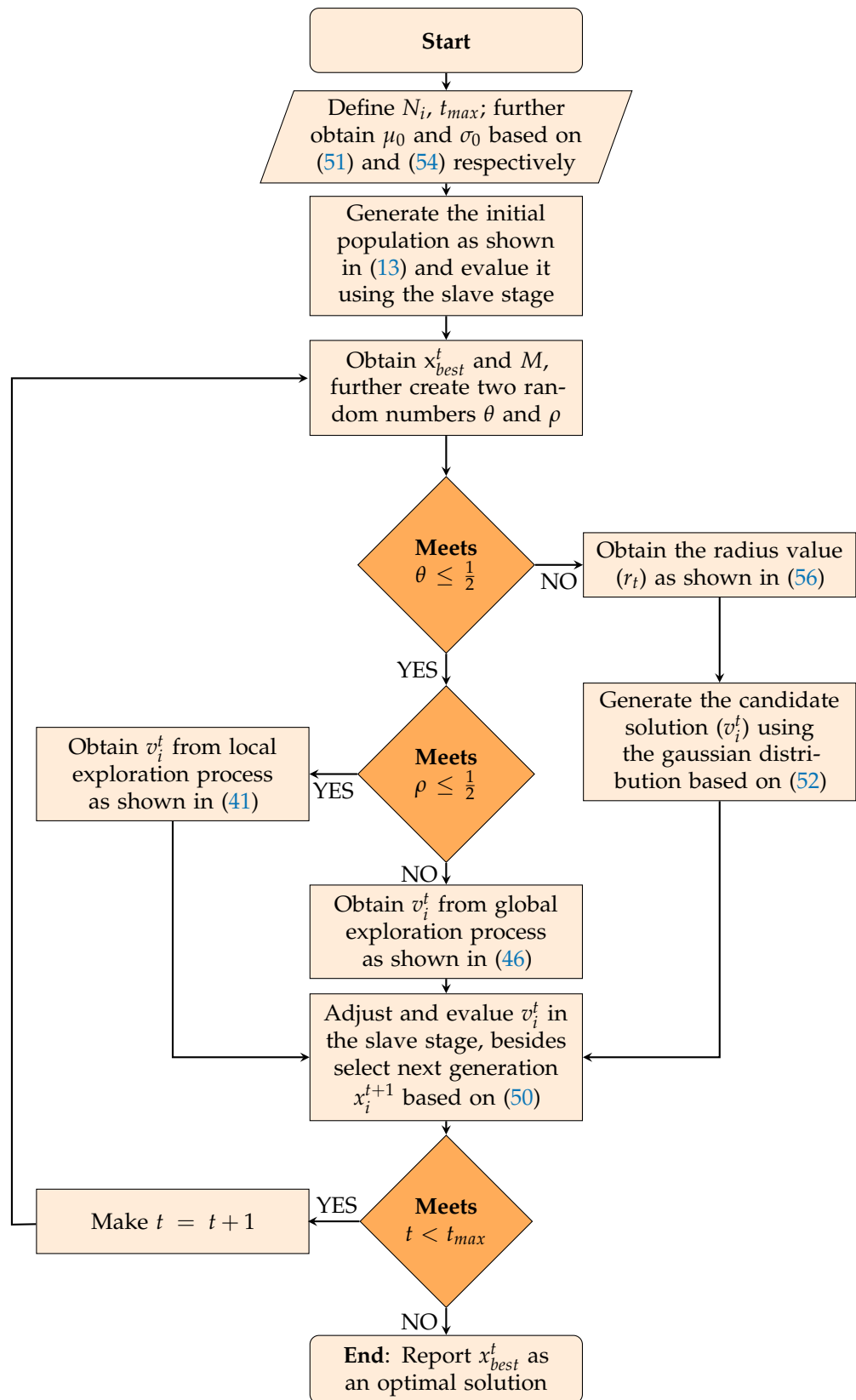
Figure 3. Flowchart used for the improved GNDO.

Algorithm 1. Improved implementation of the GNDO based on the VSA.

Data: Select the AC electrical network under study;
Find the equivalent electrical network in values per unit;
Assign the population size (N_i), the maximum iterations (t_{max}) and $t = 0$;
Find the initial center (μ_0) and the standard desviation (σ_0) as shown in (51) and (54), respectively;
Generate the initial population according to (13);
Establish the best adaptive initial function as $A_f(x_{best}^t) = \infty$;
for $t \leq t_{max}$ **do**
    Obtain the value of the objective function for each of the individuals belonging to the initial
    population x_i^t with the help of the slave stage;
    Select the individual x_{best}^t as the one that obtains the minimum value in the objective function
    according to the results found in $A_f(x_i^t)$;
    for $i = 1 : N_i$ **do**
        Generate two random numbers ϑ and ϱ between 0 and 1;
        Enter the value of the vector M as described in (45);
        if $\vartheta < \frac{1}{2}$ **then**
            Generate three random numbers j, k and m with each of them different from each other
            and different from i;
            Find the value of v_1 and v_2 as described in (47) and (48), respectively;
            if $\rho \leq \frac{1}{2}$ **then**
                Calculate the value of μ_i as described in (42);
                Obtain the value of δ_i as described in (43);
                Find the penalty factor η according to (44);
                Obtain v_i^t as described in (41);
            Else
                Perform the global exploration process as explained in (46);
            End
            Verify and adjust the values of v_i^t according to the limits established in (49);
            Evaluate v_i^t in the slave stage in order to obtain the value of the objective function
            $A_f(v_i^t)$;
            Select next generation x_i^{t+1} as explained in (50);
        Else
            Obtain the radius r_t as expressed in (56);
            Generate the candidate solutions using the Gaussian distribution with center at μ_t
            based on (52);
            Verify and adjust the values of v_i^t according to the limits established in (49);
            Evaluate v_i^t in the slave stage in order to obtain the value of the objective function
            $A_f(v_i^t)$;
            Select next generation x_i^{t+1} as explained in (50);
        End
    End
End

---

5. Characteristics of the Test Systems

In this section, two different radial distribution systems composed of 8 and 27 buses are presented. The test systems will be analyzed under two study scenarios. The first case corresponds to the analysis of the test systems operating under balanced loads, while the second case corresponds to the analysis of the test systems operating under unbalanced loads [26]. For both radial distribution systems, Star connections are used for all loads. The general operating parameters for both test systems are listed in Table 3.

Table 3. General simulation parameters.

Parameter	Value	Unit
Energy cost	0.1390	(US$/kWh)
Iterations	1000	-
Population size	30	-
Tolerance	1×10^{-10}	-

5.1. First Test System

This first test system is a three-phase electrical distribution network consisting of 7 lines and 8 buses operating at an average nominal voltage of 13.8 kV between phase and neutral with a unity power factor. Due to its radial topology, the slack bus corresponds to bus 1 [26]. The electrical network is presented in Figure 4.
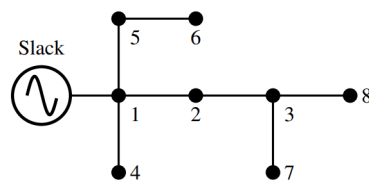
Figure 4. Single-line diagram for the 8-bus test system.

Table 4 shows the corresponding information for the case of operating under a balanced load scenario for the 8-bus system. It also presents the length for each network section, the load levels per phase present for each load bus (PQ) bus and the topology of the electrical network.

Table 4. Information corresponding to the 8-bus test system for the balanced case.

Line	Bus i	Bus j	L_{ij} (km)	$P_{j,h}^D$ (kW)	$Q_{j,h}^D$ (kvar)
1	1	2	1.00	1054.2	0
2	2	3	1.00	806.5	0
3	1	4	1.00	2632.5	0
4	1	5	1.00	609	0
5	5	6	1.00	2034.5	0
6	3	7	1.00	932.8	0
7	3	8	1.00	1731.4	0

Table 5 shows the corresponding information for the case of operating under an unbalanced load scenario for the 8-bus system, in which the different load levels per phase present for each PQ bus are shown.

Table 5. Information corresponding to the 8-bus test system for the unbalanced case.

Bus j	$P_{j,a}^D$ (kW)	$Q_{j,a}^D$ (kvar)	$P_{j,b}^D$ (kW)	$Q_{j,b}^D$ (kvar)	$P_{j,c}^D$ (kW)	$Q_{j,c}^D$ (kvar)
2	3162.6	0	0	0	0	0
3	0	0	2419.5	0	0	0
4	0	0	0	0	7897.5	0
5	913.5	0	913.5	0	0	0
6	0	0	3051.6	0	3051.6	0
7	2798.4	0	0	0	0	0
8	1298.55	0	2597.1	0	1298.55	0

5.2. Second Test System

This second test system is a three-phase electrical distribution network made up of 26 lines and 27 buses operating at an average nominal voltage of 13.8 kV between phase and neutral with a unitary power factor. Due to its radial topology, the slack bus corresponds to bus 1 [26]. The electrical network is presented in Figure 5.
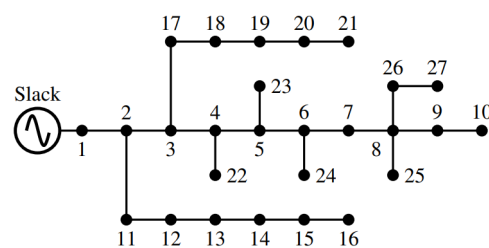

Figure 5. Single-line diagram for the 27-bus test system.

Table 6 shows the corresponding information for the case of operating under a balanced load scenario for the 27-bus system, in which the length for each network section and the load levels per phase present for each PQ bus and the topology of the electrical network are shown.

Table 6. Information corresponding to the 27-bus test system for the balanced case.

Line	Bus i	Bus j	$L_{i,j}$ (km)	$P^D_{j,h}$ (kW)	$Q^D_{j,h}$ (kvar)
1	1	2	0.55	0	0
2	2	3	1.50	0	0
3	3	4	0.45	297.5	184.4
4	4	5	0.63	0	0
5	5	6	0.70	255	158
6	6	7	0.55	0	0
7	7	8	1.00	212.5	131.7
8	8	9	1.25	0	0
9	9	10	1.00	266.1	164.9
10	2	11	1.00	85	52.7
11	11	12	1.23	340	210.7
12	12	13	0.75	297.5	184.4
13	13	14	0.56	191.3	118.5
14	14	15	1.00	106.3	65.8
15	15	16	1.00	255	158
16	3	17	1.00	255	158
17	17	18	0.60	127.5	79
18	18	19	0.90	297.5	184.4
19	19	20	0.95	340	210.7
20	20	21	1.00	85	52.7
21	4	22	1.00	106.3	65.8
22	5	23	1.00	55.3	34.2
23	6	24	0.40	69.7	43.2
24	8	25	0.60	255	158
25	8	26	0.60	63.8	39.5
26	26	27	0.80	170	105.4

Table 7 shows the corresponding information for the case of operating under an unbalanced load scenario for the 27-bus system, in which the different load levels per phase present for each PQ bus are shown.

Table 7. Information corresponding to the 27-bus test system for the unbalanced case.

Bus j	$P^D_{j,a}$ (kW)	$Q^D_{j,a}$ (kvar)	$P^D_{j,b}$ (kW)	$Q^D_{j,b}$ (kvar)	$P^D_{j,c}$ (kW)	$Q^D_{j,c}$ (kvar)
2	0	0	0	0	0	0
3	0	0	0	0	0	0
4	892.5	553.2	0	0	0	0
5	0	0	0	0	0	0
6	0	0	765	474	0	0
7	0	0	0	0	0	0
8	0	0	0	0	637.5	395.1
9	0	0	0	0	0	0
10	0	0	0	0	798.3	494.7
11	0	0	255	158.1	0	0
12	1020	632.1	0	0	0	0
13	446.25	276.6	446.25	276.6	0	0
14	0	0	286.95	177.75	286.95	177.75
15	159.45	98.7	0	0	159.45	98.7
16	0	0	382.5	237	382.5	237
17	1	0	765	474	0	0
18	382.5	237	0	0	0	0
19	446.25	276.6	446.25	276.6	0	0
20	0	0	510	316.05	510	316.05
21	127.5	79.05	0	0	127.5	79.05
22	0	0	159.75	98.7	159.75	98.7
23	165.9	102.6	0	0	0	0
24	0	0	0	0	209.1	129.6
25	255	158	255	158	255	158
26	63.8	39.5	63.8	39.5	63.8	39.5
27	170	105.4	170	105.4	170	105.4

5.3. Set of Available Conductors

Eight different types of conductors are considered to be assigned within the different test systems exposed. Table 8 shows the different values of impedances, maximum thermal currents and cost per kilometer for each of them.

Table 8. Set of conductors considered for the different test systems.

Gauge (c)	r (Ω/km)	x (Ω/km)	$I^{c,max}$ (A)	C^c (US\$/km)
1	0.8763	0.4133	180	1986
2	0.6960	0.4133	200	2790
3	0.5518	0.4077	230	3815
4	0.4387	0.3983	270	5090
5	0.3480	0.3899	300	8067
6	0.2765	0.3610	340	12,673
7	0.0966	0.1201	600	23,419
8	0.0853	0.0950	720	30,070

6. Computational Validation

The proposed optimization methodology is implemented on a personal computer using MATLAB® R2021a software. The computer has an Intel (R) Core (TM) i7-8565U CPU @1.80 GHz 1.99 GHz, 8 Gb RAM (Intel, Santa Clara, CA, USA), and Windows 11 Home operating system of $\times$64 bits. The results are analyzed with the help of Microsoft Power BI Desktop® Version 2.109.642.0 $\times$64 bits (Redmond, WA, USA).

7. Results and Discussion

This section presents the numerical results obtained for both test systems considering an operating scenario in peak demand, i.e., $T = 8760$ h and with demand of 100% at every instant of time.

7.1. Results in a Balanced Operating Scenario

The results obtained for IEEE 8 and 27-bus test systems of are presented considering the optimization method presented with the master-slave structure for balanced operating scenarios.

7.1.1. Results in the IEEE 8-Bus Test System

Table 9 presented in [30] shows the solutions obtained by different comparative methods, such as the tabu search algorithm (TBA), traditional genetic algorithm (TGA), Chu and the Beasley genetic algorithm (CBGA), the exact MINLP solver model in General Algebraic Modeling System (GAMS), Newton's metaheuristic algorithm (NMA) and the vortex search algorithm (VSA). In the same way, the solution reached by the proposed GNDO is presented.

Table 9. Solutions obtained by different optimization methods.

Method	Gauges	Investment in Conductors (US\$)	Losses (US\$)	Annual Costs (US\$)
TGA	{6,5,3,4,4,1,4}	125,433	406,222.461	531,655.461
CBGA	{6,6,4,4,4,1,4}	143,076	373,155.965	516,231.965
GAMS	{6,4,4,5,4,1,2}	122,358	416,681.580	539,039.580
TBA	{6,5,4,4,4,1,3}	125,433	397,754.442	523,187.442
VSA	{6,6,5,5,4,2,4}	163,350	345,007.959	508,357.959
NMA	{6,6,5,5,4,2,4}	163,350	345,007.959	508,357.959
GNDO	{7,7,5,5,4,2,4}	227.826	228,143.791	455,969.791

The results presented in Table 9 show that (i) the proposed methodology based on the GNDO improves the numerical results obtained by the NMA and discrete version of the VSA (DVSA) algorithms, with a solution equal to US \$ 455,969,791, of which 50.03% corresponds to the costs associated with energy losses stipulated for the established planning

horizon and 49.97% corresponds to the costs associated with the investment in conductors. (ii) The second-best solution methodology is the NMA and DVSA algorithms, both with an objective function value equivalent to US\$ 508,357,959, followed in third place by the CBGA solution methodology with an objective function value of US\$ 516,231,965. (iii) It is noted how the solution obtained by the GNDO presents the highest level of investment in conductors compared to the other methods. However, this increase in the investment cost is compensated by a lower level of cost in energy losses, so in that sense the best combination of gauges is achieved for this test system. (iv) The proposed methodology based on the GNDO reduces annual costs by 10.30% compared to the second-best solution presented in Table 9.

In contrast, Figure 6 shows the behavior of the voltage profiles at the eight buses of the system, where it can be observed that the minimum voltage value is present in bus six with a value of 0.9904 pu, yet it should be clarified that because the system is in a balanced load scenario, the behavior of the different voltage profiles for the different phases A, B and C will be the same.
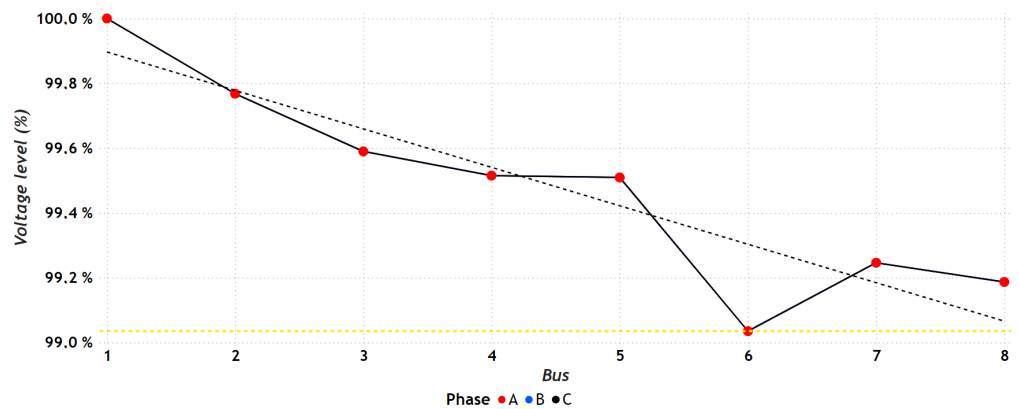
Figure 6. Behavior of the voltage profiles in the 8-bus three-phase distribution system under a balanced load scenario.

On the other hand, Figure 7 shows the total apparent power losses (S) for the phases A, B and C in the different branches belonging to the eight-bus system, it can be observed that the greatest value of losses is present in branch four with a value of 58.53 kVA. It is worth clarifying that because the system is in a balanced load scenario, the corresponding contribution of each of the phases A, B and C to the total power losses in each branch will be the same.
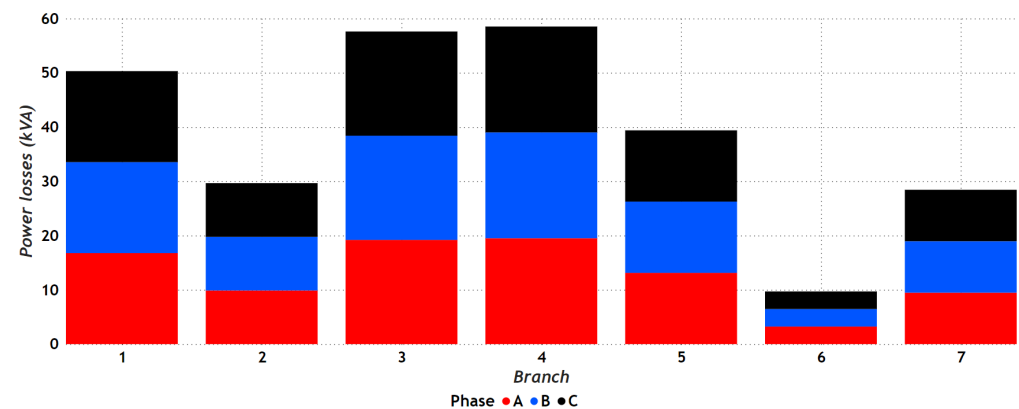
Figure 7. Power losses present in the branches of the three-phase 8-bus distribution system under a balanced load scenario.

Finally, Figure 8 represents the loadability of each of the branches in the 8-bus system, which shows the comparison between the maximum current value obtained from the

phases A, B and C for a given branch X against the maximum-established current limits according to gauge-type obtained for said network section shown in Table 8. In this way, it is important to highlight that the maximum flowing currents for each of the branches are quite far from the limits of the established maximum current.
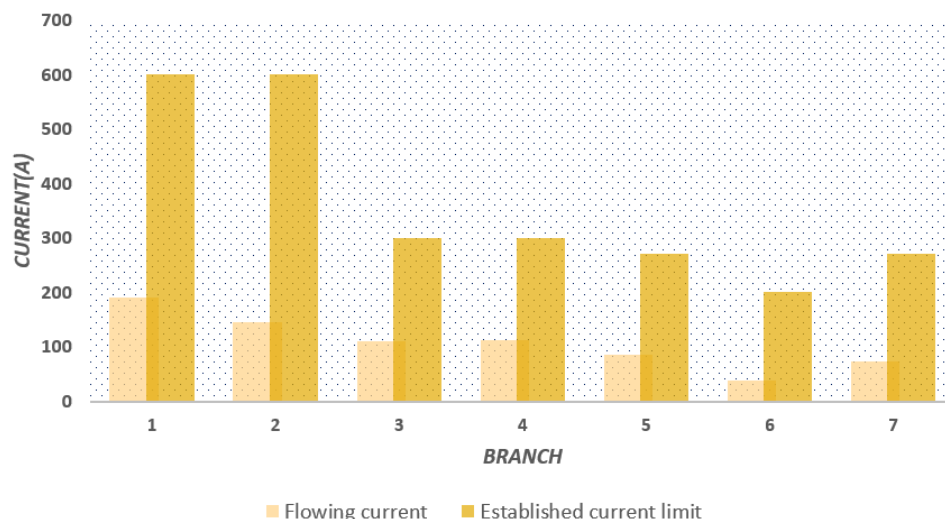

Figure 8. Loadability levels present in the branches of the three-phase 8-bus distribution system under a balanced load scenario.

7.1.2. Results in the IEEE 27-Bus Test Scenario

In Table 10 presented in [30] the results obtained by different comparative methods are presented, such as the vortex search algorithm (VSA) and Newton's metaheuristic algorithm (NMA). In the same way, the solution reached by the proposed GNDO is presented.

Table 10. Solutions obtained by different optimization methods.

Method	Gauges	Investment in Conductors (US$)	Losses (US$)	Annual Costs (US$)
VSA	{7,7,5,4,4,3,3,1,1,4,4,2,3 2,1,4,4,2,2,2,1,1,2,2,1,1}	344,352.150	217,672.327	562,024.477
NMA	{7,7,4,4,4,4,3,1,1,4,4,3,3 1,2,4,3,2,1,1,1,1,2,2,1,1}	337,744.800	219,950.455	557,695.255
GNDO	{7,7,4,4,4,3,3,1,1,4,4,2,1 1,1,3,2,2,1,1,1,1,1,1,1,1}	319,768.08	230,115.492	549,883.572

The results presented in Table 10 show that (i) the proposed methodology based on the GNDO improves the numerical results obtained by the NMA and DVSA algorithms, with a solution equal to US $ 549,883.572, of which 41.85% corresponds to the costs associated with the energy losses stipulated for the established planning horizon and 58.15% corresponds to the costs associated with the investment in conductors; (ii) It is noted how the solution obtained by the GNDO presents the lowest level of investment in conductors compared to the other methods. However, this lower investment cost promotes an increase in the cost of energy losses, so, although there is a slight increase in the latter, it is not high enough, so the lowest value of the objective function is obtained when compared with the objective functions of the different methods shown in Table 10. In this sense, the best combination of gauges is achieved for this test system. (iii) The GNDO methodology reduces annual costs by 1.40% with respect to the second-best solution presented in Table 10.

In contrast, Figure 9 shows the behavior of the voltage profiles in the 27 buses of the system, where it can be observed that the minimum voltage value is present in bus 10 with a value of 0.9771 pu, and should be clarified that because the system is in a balanced load

scenario, the behavior of the different voltage profiles for the different phases A, B and C will be the same.
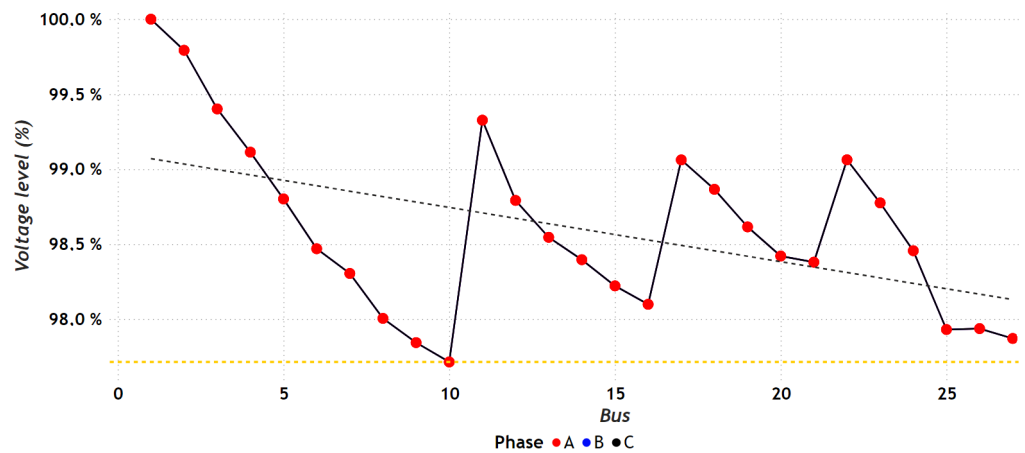

Figure 9. Behavior of the voltage profiles in the three-phase 27-bus distribution system under a balanced load scenario.

On the other hand, Figure 10 shows the total apparent power losses (S) for the phases A, B and C in the different branches belonging to the 27-bus system, it can be observed that the highest losses occur in branch two with a value of 42.42 kVA. Because the system is in a balanced load scenario, the corresponding contribution of each of the phases A, B and C to the total power losses in each branch will be the same.
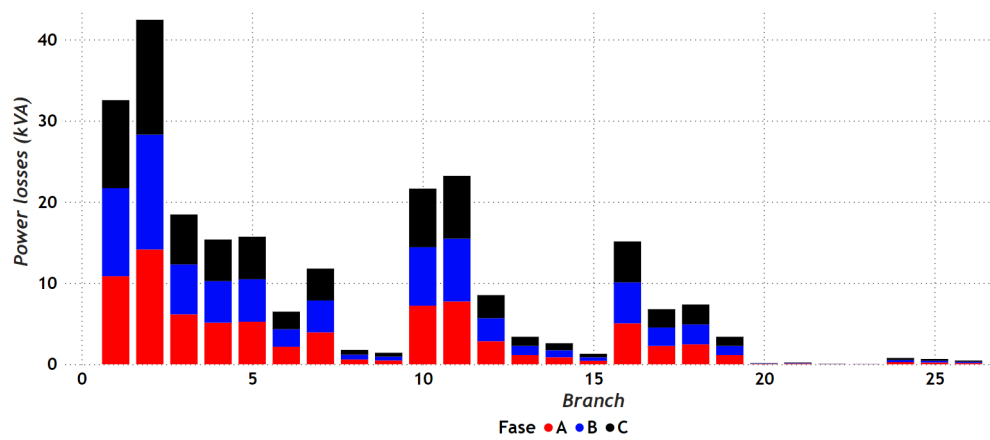
Figure 10. Power losses present in the branches of the three-phase 27-bus distribution system under a balanced load scenario.

Finally, Figure 11 represents the loadability of each of the branches in the 27-bus system, which shows the comparison between the maximum current value obtained from the phases A, B and C for a given branch X against the maximum-established current limits according to gauge-type obtained for said network section shown in Table 8. In this way, it is important to highlight that the maximum flowing currents for each of the branches are quite far from the limits of the established maximum current.
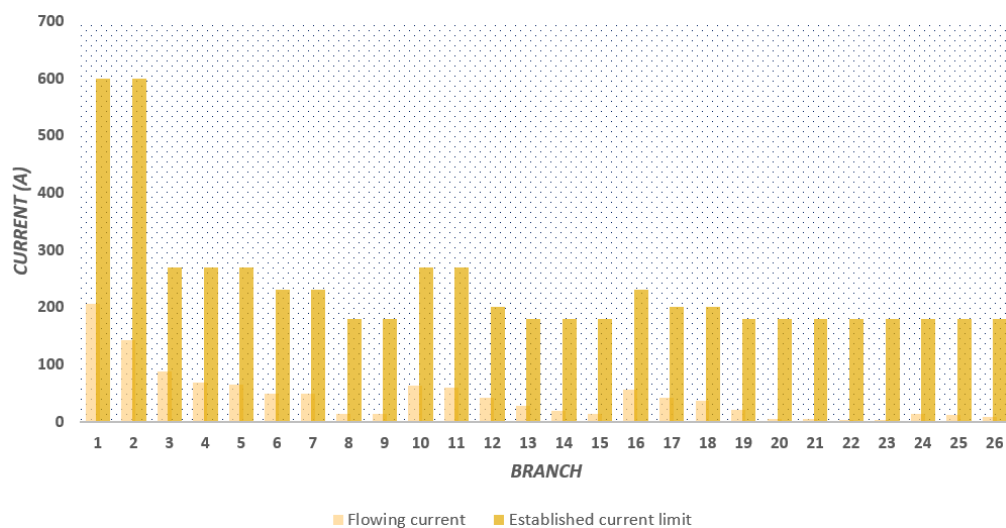
Figure 11. Country house with poor lighting.

7.2. Results in an Unbalanced Operating Scenario

The results obtained for IEEE 8- and 27-bus test systems are presented considering the optimization method used with master-slave structure for the unbalanced operating scenarios.

7.2.1. Results in the IEEE 8-Bus Test System

Table 11 presented in [30] shows the results obtained by different comparative methods, such as the vortex search algorithm (VSA) and Newton's metaheuristic algorithm (NMA). In the same way, the solution reached by the proposed GNDO is presented.

Table 11. Solutions obtained by different optimization methods.

Method	Gauges	Investment in Conductors (US$)	Losses (US$)	Annual Costs (US$)
VSA	{7,7,7,5,5,4,4}	289,713	269,045.394	558,758.394
NMA	{7,7,7,5,5,4,4}	289,713	269,045.394	558,758.394
GNDO	{7,7,7,5,5,4,4}	289,713	269,045.394	558,758.394

The results presented in Table 11 show that (i) the proposed methodology based on the GNDO does not improve but matches the numerical results obtained by the NMA and VSA algorithms because a solution equal to US $ 558,758.394 is obtained, of which 48.15% corresponds to the costs associated with the energy losses stipulated for the established planning horizon and 51.85% corresponds to the costs associated with the investment in conductors.

In contrast, Figure 12 shows the behavior of the voltage profiles in the eight buses of the system, where it can be observed that the minimum voltage value is present in bus six for the phase B with a value of 0.9869 pu, it should be noted that because the system is in an unbalanced load scenario, the behavior of the different voltage profiles for the different phases A, B and C will no longer be the same.
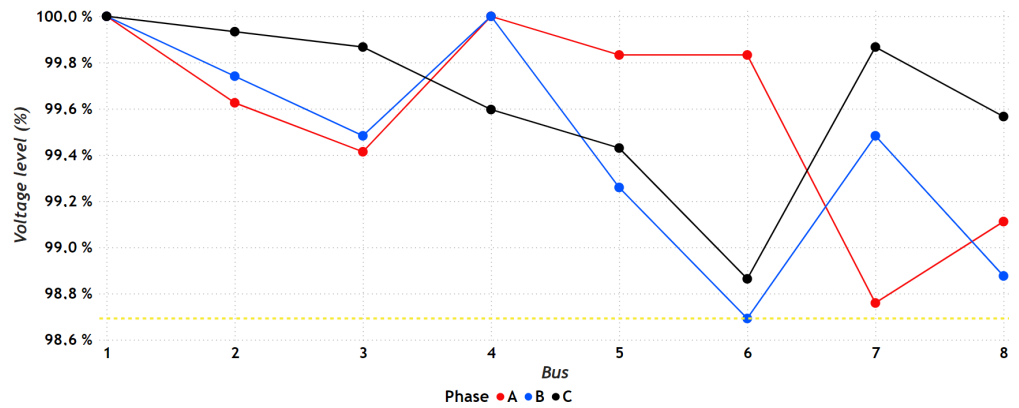
Figure 12. Behavior of the voltage profiles in the three-phase 8-bus distribution system under an unbalanced load scenario.

On the other hand, Figure 13 shows the total apparent power losses (S) for the phases A, B and C in the different branches belonging to the eight-bus system. It can be observed that the highest losses value is present in branch three in phase C with a value of 50.89 kVA. It should be clarified that because the system is in an unbalanced load scenario, the corresponding contribution of each of the phases A, B and C to the total power losses in each branch will no longer be the same.
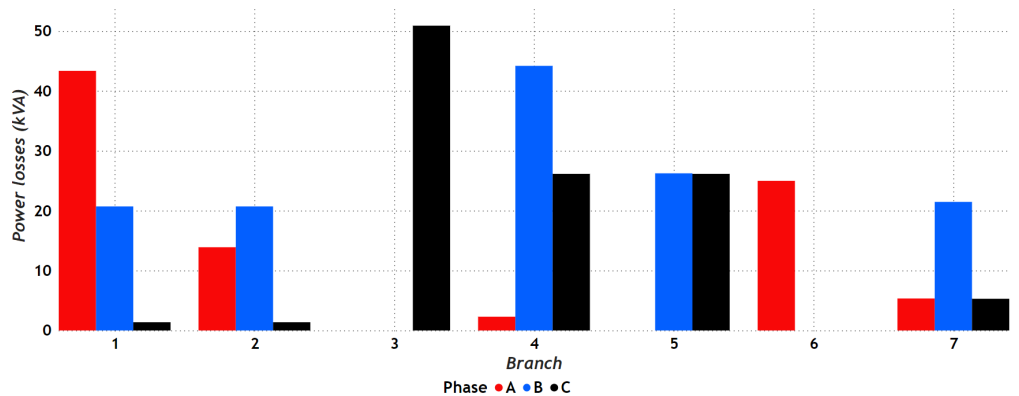
Figure 13. Power losses present in the branches of the three-phase 8-bus distribution system under an unbalanced load scenario.

Finally, Figure 14 represents the loadability of each of the branches in the 8-bus system, which shows the comparison between the maximum current value obtained of phases A, B and C for a given branch X against the maximum-established current limits according to gauge-type obtained for said network section shown in Table 8. In this way, it is important to highlight that the maximum flowing currents for each of the branches are quite far from the limits of the established maximum current.
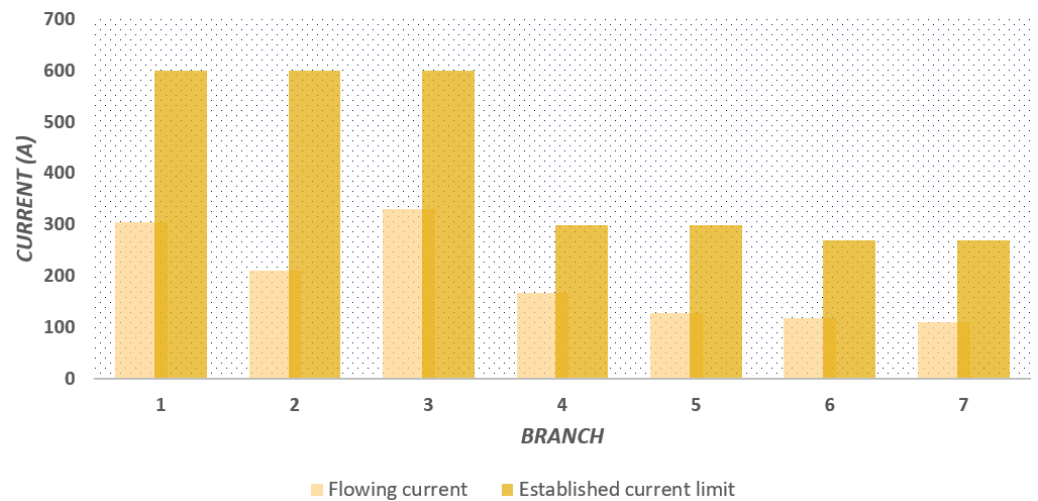
Figure 14. Loadability levels present in the branches of the three-phase 8-bus distribution system under an unbalanced load scenario.

7.2.2. Results in the IEEE 27-Bus Test Scenario

Table 12 presented in [30] shows results obtained by different comparative methods, such as the vortex search algorithm (VSA) and Newton's metaheuristic algorithm (NMA). In the same way, the solution reached by the proposed GNDO is presented.

Table 12. Solutions obtained by different optimization methods.

Method	Gauges	Investment in Conductors (US$)	Losses (US$)	Annual Costs (US$)
VSA	{7,7,5,4,4,4,4,2,2,4,4,3,2 1,1,2,3,2,1,2,2,1,2,2,4,1}	350,392.95	257,999.185	608,392.135
NMA	{7,7,4,4,4,3,4,2,1,4,4,4,2 1,1,4,3,2,2,1,1,1,2,2,2,1}	344,954.40	252,624.608	597,579.008
GNDO	{7,7,4,4,4,4,4,1,1,4,4,3,1 1,1,4,2,2,1,1,1,1,1,1,1,1}	331,828.08	257,190.720	589,018.800

The results presented in Table 12 show that (i) the proposed methodology based on the GNDO improves the numerical results obtained by the NMA and DVSA algorithms, with a solution equal to US $ 589,018,800, of which 43.66% corresponds to the costs associated with the energy losses stipulated for the established planning horizon and 56.34% corresponds to the costs associated with the investment in conductors; (ii) It is indicated how the solution obtained by the GNDO presents the lowest investment in conductors compared to the other methods. However, this lower investment cost promotes an increase in the cost of energy losses, so, although there is a slight increase in the latter, it is not high enough, so the lowest value of the objective function is obtained when compared with the objective functions of the different methods presented in Table 12. In this sense, the best combination of gauges is achieved for this test system. (iii) The proposed methodology based on the GNDO reduces annual costs by 1.43% compared to the second-best solution presented in Table 12.

In contrast, Figure 15 shows the behavior of the voltage profiles in the 27 buses of the system, where it can be observed that the minimum voltage value is present in bus 10 for phase C with a value of 0.9596 pu. This is due to the active and reactive power demand value present in bus 10 for phase C, with values of 798.3 kW and 497.7 kvar, respectively, which constitute the highest demand values for this phase in all the buses of the distribution system in the unbalanced scenario. In this sense, by comparing phases A, B and C, it can be seen that, since the first two lack demand, their behavior with respect to phase C remains more stable. In the same way, when performing a topological analysis of the network, it is possible to observe that bus 10 is one of the furthest nodes from the slack node, which

entails more significant voltage variations. It should be clarified that because the system is in an unbalanced load scenario, the behavior of the different voltage profiles for the different phases A, B and C is not the same.
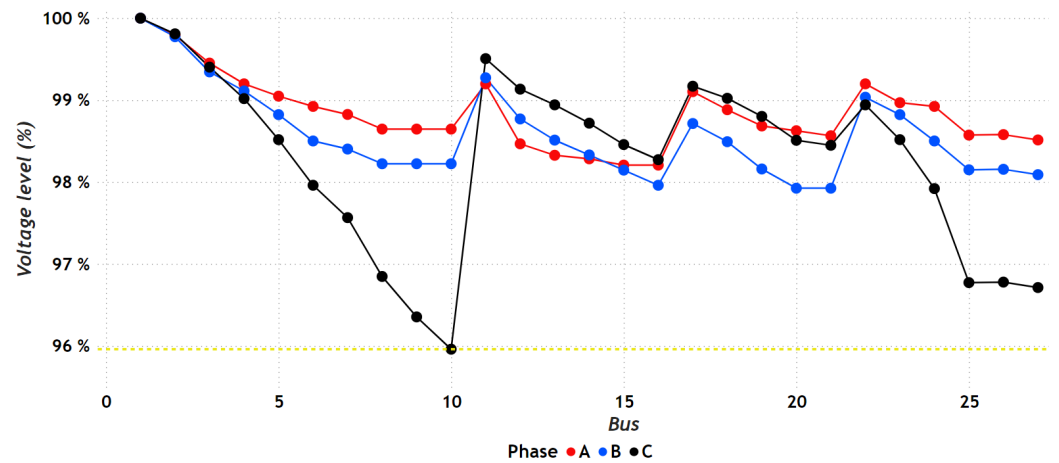

Figure 15. Behavior of the voltage profiles in the three-phase 27-bus distribution system under an unbal-anced load scenario.

On the other hand, Figure 16 shows the total apparent power losses (S) for the phases A, B and C in the different branches belonging to the 27-bus system; it can be observed that the greatest losses are present in phase B for branch two with a value of 17.06 kVA and in phase C for branch seven with a value of 17.15 kVA. It is valid to clarify that because the system is in an unbalanced load scenario, the contribution corresponding to phases A, B, and C to the total power losses in each branch will no longer be the same.
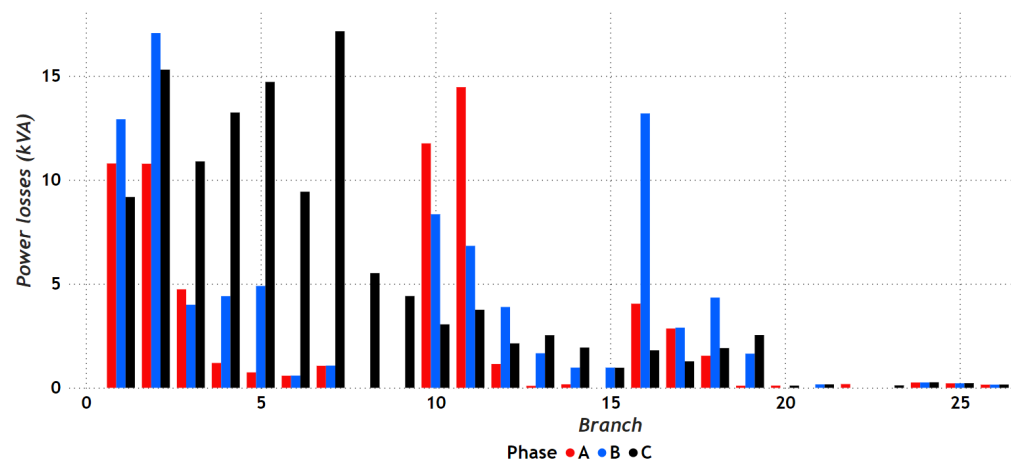
Figure 16. Power losses present in the branches of the three-phase 27-bus distribution system under an unbalanced load scenario.

Finally, Figure 17 represents the loadability of each of the branches in the 27-bus system, which shows the comparison between the maximum current value obtained of phases A, B and C for a given branch X against the maximum-established current limits according to gauge-type obtained for said network section shown in Table 8. In this way, it is important to highlight that the maximum flowing currents for each of the branches are pretty far from the limits of the established maximum current.
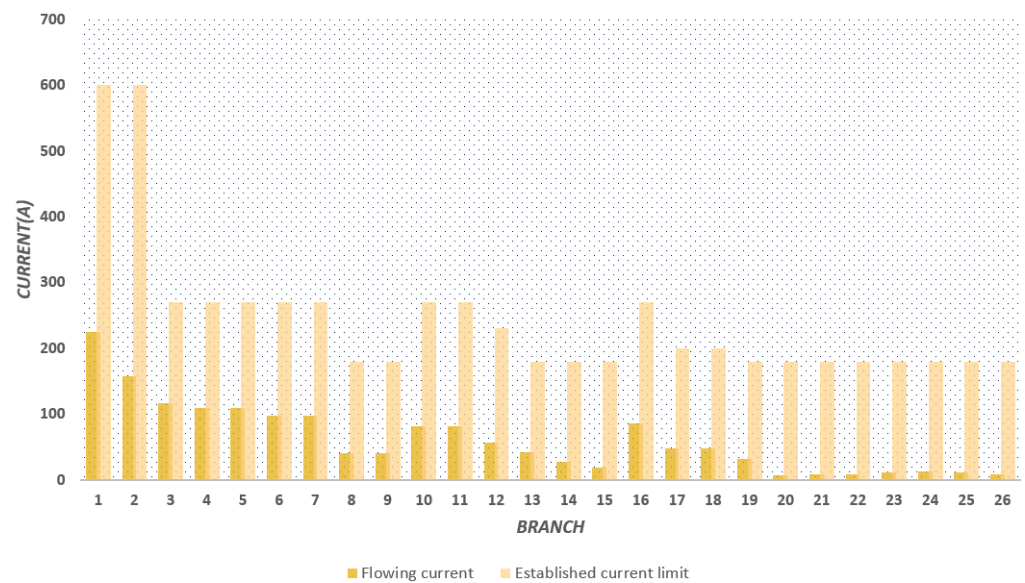
Figure 17. Loadability levels present in the branches of the three-phase 27-bus distribution system under an unbalanced load scenario.

7.3. Complementary Analysis

To analyze the behavior of the proposed algorithm, Figures 18 and 19 are shown. These results show how the proposed GNDO algorithm behaved in the search to minimize the value of the objective function throughout all iterations (t_{max}). It is observed how the IEEE 8-bus system for both balanced and unbalanced loads manages to converge and stabilize in a few iterations; on the other hand, the IEEE 27-bus system for both balanced and unbalanced loads takes many more iterations (t) to converge.

In the same way, according to the results obtained from the IEEE 8- and 27-bus systems for the test scenarios under balanced and unbalanced loads, the following is obtained:

- The proposed GNDO only needs a single evaluation to obtain the numerical results presented in this research, which guarantees very reduced computation times, making this algorithm the most efficient one reported in the specialized literature.
- The proposed GNDO improves the results in most of the case studies presented, with the exception of the 8-bus test system under an unbalanced operating scenario, in which it matches the results obtained by algorithms such as the NMA or the VSA. In this way, it can be inferred that for this particular case study, the overall optimal solution has been obtained.
- The levels of loadability shown for each of the lines in the different cases of study guarantee good functioning in the electrical distribution systems tested, additionally ensuring the possibility of future expansions and new load connections.
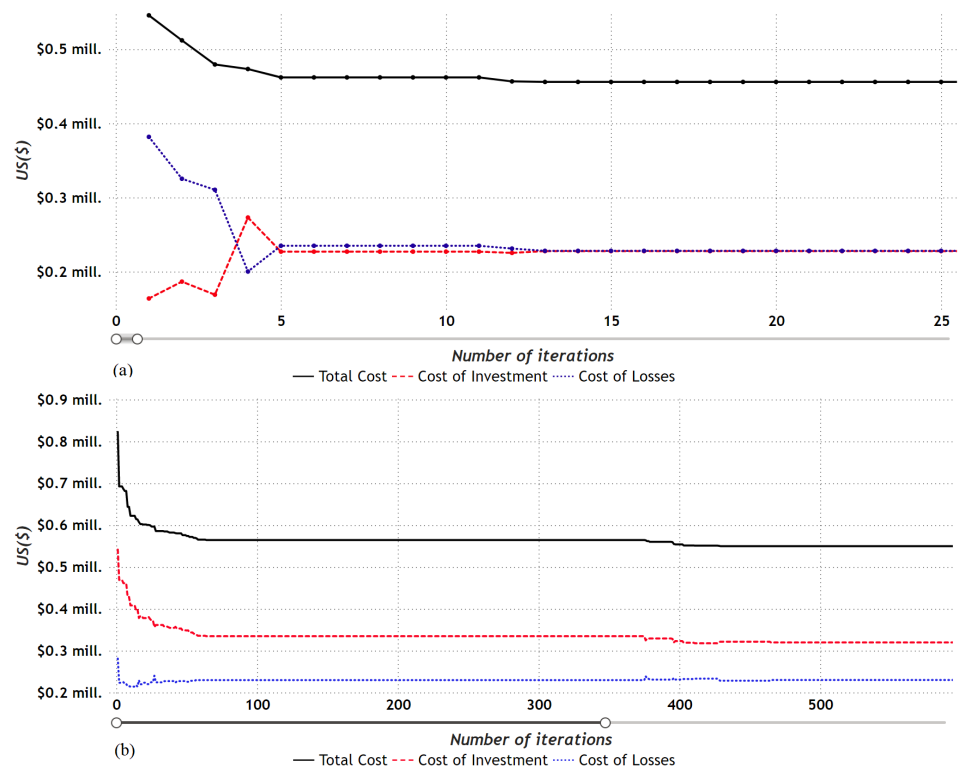
Figure 18. Behavior of the value of the objective function for: (**a**) 8-bus system with balanced load; (**b**) 27-bus system with balanced load.
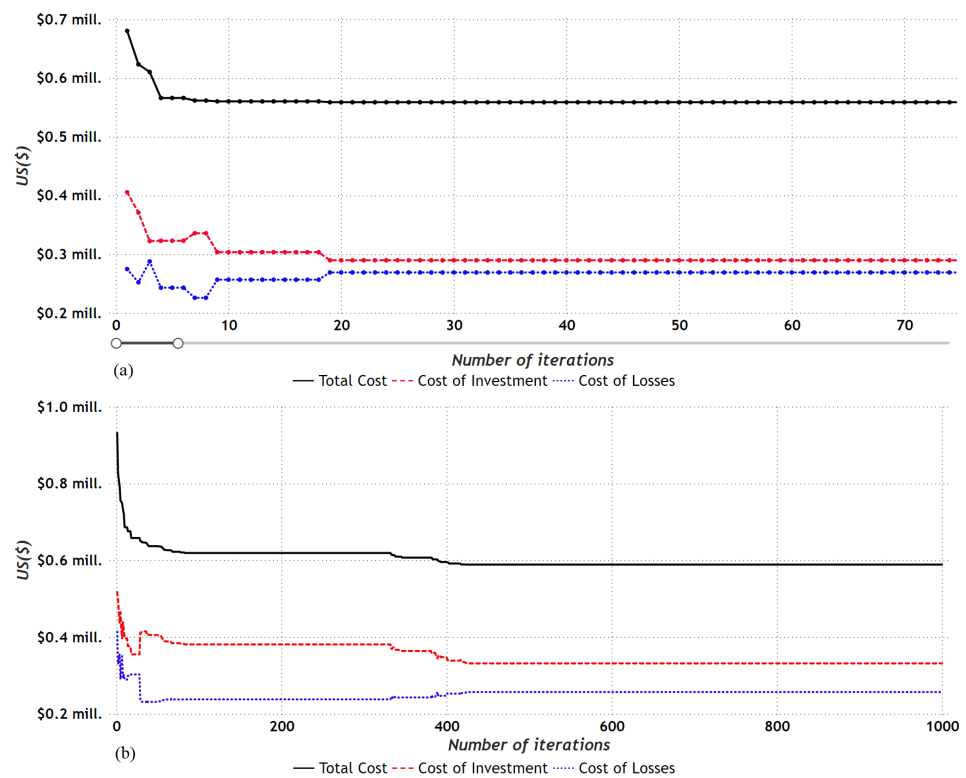

Figure 19. Behavior of the value of the objective function for: (**a**) 8-bus system with unbalanced load; (**b**) 27-bus system with unbalanced load.

7.4. Selection of Conductors Considering Different Load Periods

To validate the effectiveness of the proposed GNDO in dealing with medium-scale distribution networks considering demand variations, this subsection presents some numerical validations for the three-phase asymmetric version of the IEEE 33-bus grid. It´s single line diagram is presented in Figure 20. The nodal connections and the line lengths are listed in Table 13.
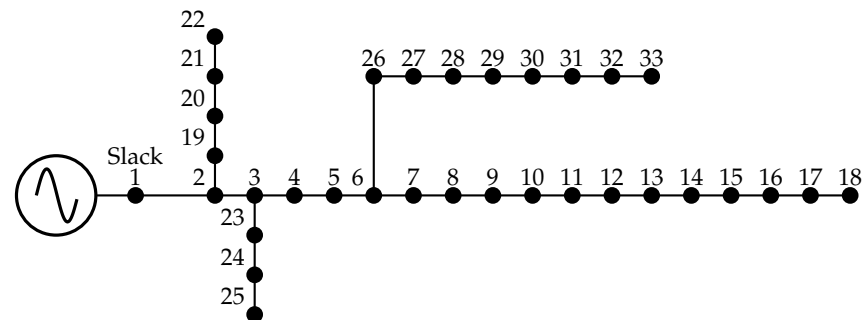

Figure 20. IEEE 33-bus single line diagram.

Table 13. Information corresponding to the 33-bus test system.

Line	Bus i	Bus j	L_{ij} (km)
1	1	2	0.0699
2	2	3	0.3720
3	3	4	0.2762
4	4	5	0.2876
5	5	6	0.7630
6	6	7	0.4030
7	7	8	1.4733
8	8	9	0.8850
9	9	10	0.8900
10	10	11	0.1308
11	11	12	0.2491
12	12	13	1.3115
13	13	14	0.6272
14	14	15	0.5585
15	15	16	0.6457
16	16	17	1.5050
17	17	18	0.6530
18	2	19	0.1603
19	19	20	1.4298
20	20	21	0.4439
21	21	22	0.8231
22	3	23	0.3798
23	23	24	0.8035
24	24	25	0.7985
25	6	26	0.1532
26	26	27	0.2145
27	27	28	0.9963
28	28	29	0.7524
29	29	30	0.3830
30	30	31	0.9687
31	31	32	0.3362
32	32	33	0.4356

The information regarding power consumption per node in the three-phase version of the 33-bus grid is listed in Table 14.

Table 14. Information corresponding to the 33-bus test system.

Bus j	$P_{j,a}^D$ (kW)	$Q_{j,a}^D$ (kvar)	$P_{j,b}^D$ (kW)	$Q_{j,b}^D$ (kvar)	$P_{j,c}^D$ (kW)	$Q_{j,c}^D$ (kvar)
2	100	50	100	60	0	0
3	90	0	90	40	0	0
4	120	75	120	80	150	90
5	60	20	60	30	60	30
6	60	18	60	20	60	20
7	200	150	0	0	100	100
8	200	0	200	100	0	0
9	60	60	0	0	0	0
10	60	60	60	20	0	0
11	45	30	45	30	45	30
12	0	0	60	35	155	100
13	60	110	60	35	60	35
14	120	80	190	80	120	80
15	60	10	60	50	60	10
16	60	20	110	80	60	20
17	60	20	150	95	0	0
18	90	40	100	0	90	40
19	0	0	0	0	90	40
20	210	50	85	40	70	75
21	90	40	110	40	110	20
22	300	400	0	0	90	40
23	90	50	70	0	0	0
24	420	200	420	200	420	200
25	120	75	0	0	150	100
26	60	25	80	25	0	0
27	0	0	80	25	0	0
28	60	20	48	24	60	20
29	120	70	185	75	120	70
30	200	600	400	400	500	600
31	150	70	120	90	150	70
32	210	100	120	35	210	100
33	60	40	100	750	0	0

To evaluate the effectiveness of the proposed GNDO in solving the problem of the optimal selection of conductors in three-phase unbalanced distribution networks against different demand variations, three numerical validations are carried out, as defined below.

- Case 1: The evaluation of the optimization methodology during the peak load condition, condition, i.e., under the same simulation conditions used for the 8- and 27-bus grids.
- Case 2: The evaluation of the optimization methodology considering daily load variations, according to Table 15 data.
- Case 3: The evaluation of the optimization methodology considering three different demand periods over the year as follows: (i) 1000 h at 100 percent demand, (ii) 6760 h at 60 percent demand, (iii) 1000 h at 30 percent demand.

Table 15. Daily demand variation for the 33-bus grid.

Time (h)	Demand (pu)	Time (h)	Demand (pu)	Time (h)	Demand (pu)
1	0.684511335492475	9	0.706039245570585	17	0.874071251666984
2	0.644122690036197	10	0.787007048961707	18	1
3	0.613069156029720	11	0.839016955610593	19	0.983615926843208
4	0.599733282530006	12	0.852733854067441	20	0.936368832158506
5	0.588874071251667	13	0.870642027052772	21	0.887597637645266
6	0.598018670222900	14	0.834254143646409	22	0.809297008954087
7	0.626786054486569	15	0.816536483139646	23	0.745856353591160
8	0.651743189178891	16	0.819394170318156	24	0.733473042484283

Note that no comparison with the previous literature reports is made in this simulation scenario since this is the first time that the IEEE 33-bus grid is adapted to a three-phase unbalanced version of studying the problem of the optimal selection of conductors. This

implies that the results reported here will become a reference for future developments in this research area.

Table 16 presents the list of calibers assigned for each operative scenario. The main characteristic of the conductors selected for each operative scenario is that these solutions fulfill the telescopic operating condition typically implemented by distribution companies to reduce investment costs in conducting material.

Table 16. Conductors selected for the IEEE 33-bus grid at each operative scenario.

Line	Case 1	Case 2	Case 3
1	7	4	7
2	7	4	7
3	7	4	7
4	7	4	7
5	7	4	7
6	7	4	7
7	7	4	7
8	7	4	7
9	7	4	7
10	7	4	7
11	7	3	6
12	7	3	6
13	7	3	4
14	6	2	4
15	5	1	1
16	5	1	1
17	1	1	1
18	4	1	5
19	4	1	2
20	4	1	1
21	1	1	1
22	5	3	4
23	5	3	4
24	1	1	1
25	7	4	7
26	7	4	5
27	6	1	5
28	6	1	3
29	6	1	3
30	3	1	1
31	2	1	1
32	2	1	1

Table 17 presents the investment, operating, and total costs for the IEEE 33-bus grid. Note that C_{pen} is zero for all the solutions listed in Table 16 since each final solution is 100% feasible.

Table 17. Investment and operating costs found with the application of the GNDO to the three-phase version of the IEEE 33-bus grid for each operative scenario.

Case	C_{inv} (USD)	C_{loss} (USD)	Z (USD)
1	814,647.151	88,991.787	903,638.938
2	195,187.456	7246.061	202,433.517
3	593,777.672	48,350.741	642,128.413

The numerical results presented in Table 17 reveal the following:

i. The investment and operating cost in Case 1, where the peak load condition is analyzed during the year, shows that to minimize the costs of energy losses, the size of the conductors is increased considerably, being this investment costs about 90.1518% of the total costs of the plan. This is an expected result since, as observed in Table 16, the solution of Case 1 has the largest conductor sizes compared with the remainder of the simulation cases.

ii. The operation scenario considering the daily load profile shows the more realistic simulation scenario (see Case 2) where the energy losses considerably reduce their costs when compared to the peak load operation scenario (about 91.8576%), which has a direct effect on the conductors selected to supply the energy load within this daily operation case. Note that the reduction in the investment costs when compared to Case 1 and Case 2 is about 76.0402%. This is an expected reduction in the investment costs since these are nonlinearly related to the energy loss costs, which implies that smaller conductor sizes can be found as an adequate balance between investment and operating costs.

iii. Case 3 shows an intermediate solution scenario between Cases 1 and 2, with a total investment of USD/year $642, 128.413$ distributed about 92.4702% on investment in conductors and 7.5298% in costs of the energy losses. Note that what happened with Case 1, the expected energy losses costs of the network, have an essential influence on the size of the conductors selected (see Table 16); in addition, note that for the distribution company, the solution in Case 3 can be the most attractive alternative since it has moderate investment costs with the main advantage that the selected conductors can support future load increments without any changes in the grid structure.

iiii. Analyzing the processing times, we obtained that for Case 1 it takes 215.5422075 seconds to converge in a single evaluation, while Case 2 and 3 take 4514.526068 and 488.239934 seconds, respectively. Based on the results obtained we can observe that Cases 1 and 2 don't represent big computational processing times, in other hand for third case its time increases among other things for daily demand variations.

8. Conclusions and Future Work

The problem of the optimal selection of conductors in asymmetric three-phase distribution networks was analyzed in this work with an improved version of the generalized normal distribution algorithm called GNDO. This algorithm included the exploration and exploitation stages based on hyper-ellipses of variable radius, which were uniformly distributed using a Gaussian distribution compared to the best current solution X^t_{best} if the parameter ϑ was greater than 50%. The numerical results show that for the 8-bus system, the proposed GNDO improves the results reported for the balanced case with a value of US \$455,969.791, on the other hand, for the unbalanced case it is the same as the reported results with a value of USD 558,758.394. In the case of the 27-bus system, the proposed GNDO improves the results reported for both the balanced case and the unbalanced case with US \$ values 549,883.572 and US \$589,018.800, respectively. This makes the proposed method the reference methodology to compare new optimization methods that are applicable to the problem of optimal selection of conductors in asymmetric three-phase distribution networks.

The processing times of the GNDO show that it takes on average 31.24 s to obtain a solution in the 8-bus system under the scenarios presented, and it takes 168.43 s on average to obtain a solution in the 27-bus system under the scenarios presented, which corresponds to extremely shorter computation times taking into account that the dimensions of the solution space for these systems are in the order of 8^7 and 8^{26} representing 2097.152 million and $3.02231454903657 \times 10^{23}$ three hundred thousand trillion possibilities.

It's notable that when the IEEE system buses increase, the processing time will increase in the same way. When comparing the processing time in the IEEE 27-bus system under peak demand and the processing time in the IEEE 33-bus system under peak demand (Case 1), it's possible to observe that it wasn't a representative incremental time. The delta value was only 47.1122 seconds. For this reason, the proposed GNDO is suitable for large-scale power grids, and its implementation doesn't have an upper limit of application.

In future works, the following works can be made: (i) apply the proposed metaheuristic methodology can be applied to solve problems associated with the local distribution system, such as the location of possible charging stations for electric vehicles, possible distributed generation, electrical compensation systems, and protection and load-balancing

devices; (ii) to apply new combinatorial optimization methods using efficient initialization algorithms for selecting conductors in large-scale distribution networks by including intelligent evolution strategies that consider the telescopic nature of the studied problem and the possibility of integrating distributed energy resources in the distribution network; and (iii) to develop a convex approximation model for the three-phase networks with a mixed-integer structure that ensure the repeatability of the solution methodology and high-quality solutions with low computational effort.

Author Contributions: Conceptualization, methodology, software, and writing (review and editing): O.D.M., J.A.V.-F. and J.S.R.-C. All authors have read and agreed to the published version of the manuscript.

References

1. Ramírez Castaño, S. *Power Distribution Networks*; Departamento de Ingeniería Eléctrica, Electrónica y Computación, Universidad Nacional de Colombia: Manizalez, Colombia, 2004. Available online: https://repositorio.unal.edu.co/handle/unal/57581 (accessed on 23 December 2022).
2. Denton, W.; Reps, D. Distribution-substation and primary-feeder planning. *Electr. Eng.* **1955**, *74*, 804–809. [CrossRef]
3. Agarwal, U.; Jain, N. Distributed energy resources and supportive methodologies for their optimal planning under modern distribution network: A review. *Technol. Econ. Smart Grids Sustain. Energy* **2019**, *4*, 1–21. [CrossRef]
4. Koziel, S.; Hilber, P.; Westerlund, P.; Shayesteh, E. Investments in data quality: Evaluating impacts of faulty data on asset management in power systems. *Appl. Energy* **2021**, *281*, 116057. [CrossRef]
5. Ahmadian, A.; Elkamel, A.; Mazouz, A. An improved hybrid particle swarm optimization and tabu search algorithm for expansion planning of large dimension electric distribution network. *Energies* **2019**, *12*, 3052. [CrossRef]
6. Kazmi, S.A.A.; Shahzad, M.K.; Khan, A.Z.; Shin, D.R. Smart distribution networks: A review of modern distribution concepts from a planning perspective. *Energies* **2017**, *10*, 501. [CrossRef]
7. Ponnavaikko, M.; Rao, K.P. Optimal distribution system planning. *IEEE Trans. Power Appar. Syst.* **1981**, *6*, 2969–2977. [CrossRef]
8. Ponnavaikko, N.; Rao, K.P.; Venkata, S. Distribution system planning through a quadratic mixed integer programming approach. *IEEE Trans. Power Deliv.* **1987**, *2*, 1157–1163. [CrossRef]
9. Adams, R.; Laughton, M. Optimal planning of power networks using mixed-integer programming. Part 1: Static and time-phased network synthesis. *Proc. Inst. Electr. Eng. IET* **1974**, *121*, 139–147. [CrossRef]
10. Islam, S.J.; Ghani, M.R.A. Economical optimization of conductor selection in planning radial distribution networks. In Proceedings of the 1999 IEEE Transmission and Distribution Conference (Cat. No. 99CH36333), New Orleans, LA, USA, 11–16 April 1999; Volume 2, pp. 858–863. [CrossRef]
11. Joshi, D.; Burada, S.; Mistry, K.D. Distribution system planning with optimal conductor selection. In Proceedings of the 2017 Recent Developments in Control, Automation & Power Engineering (RDCAPE), Noida, India, 26–27 October 2017; pp. 263–268. [CrossRef]
12. Falaghi, H.; Ramezani, M.; Haghifam, M.R.; Milani, K.R. Optimal selection of conductors in radial distribution systems with time varying load. In Proceedings of the CIRED 2005-18th International Conference and Exhibition on Electricity Distribution, Turin, Italy, 6–9 June 2005; pp. 1–4. [CrossRef]
13. Ponnavaikko, M.; Rao, K.P. An approach to optimal distribution system planning through conductor gradation. *IEEE Trans. Power Appar. Syst.* **1982**, *6*, 1735–1742. [CrossRef]

14. Mendoza, F.; Requena, D.; Bernal-Agustin, J.L.; Domínguez-Navarro, J.A. Optimal conductor size selection in radial power distribution systems using evolutionary strategies. In Proceedings of the 2006 IEEE/PES Transmission & Distribution Conference and Exposition: Latin America, Caracas, Venezuela, 15–18 August 2006; pp. 1–5. [CrossRef]

15. Legha, M.M.; Javaheri, H.; Legha, M.M. Optimal Conductor Selection in Radial Distribution Systems for Productivity Improvement Using Genetic Algorithm. *Iraqi J. Electr. Electron. Eng.* **2013**, *9*, 29–35. [CrossRef]

16. Rao, R.S.; Satish, K.; Narasimham, S. Optimal conductor size selection in distribution systems using the harmony search algorithm with a differential operator. *Electr. Power Components Syst.* **2011**, *40*, 41–56. [CrossRef]

17. Momoh, I.; Jibril, Y.; Jimoh, B.; Abubakar, A.; Ajayi, O.; Abubakar, A.; Sulaiman, S.; Yusuf, S. Effect of an optimal conductor size selection scheme for single wire earth return power distribution networks for rural electrification. *ATBU J. Sci. Technol. Educ.* **2019**, *7*, 286–295.

18. Manikandan, S.; Sasitharan, S.; Rao, J.V.; Moorthy, V. Analysis of optimal conductor selection for radial distribution systems using DPSO. In Proceedings of the 2016 3rd International Conference on Electrical Energy Systems (ICEES), Chennai, India, 17–19 March 2016; pp. 96–101. [CrossRef]

19. Kalesa, B.M. Conductor selection optimization in radial distribution system considering load growth using MDE algorithm. *World J. Model. D Simul.* **2014**, *10*, 175–184.

20. Abdelaziz, A.Y.; Fathy, A. A novel approach based on crow search algorithm for optimal selection of conductor size in radial distribution networks. *Eng. Sci. Technol. Int. J.* **2017**, *20*, 391–402. [CrossRef]

21. Ismael, S.M.; Aleem, S.H.A.; Abdelaziz, A.Y. Optimal selection of conductors in Egyptian radial distribution systems using sine-cosine optimization algorithm. In Proceedings of the 2017 Nineteenth International Middle East Power Systems Conference (MEPCON), Cairo, Egypt, 19–21 December 2017; pp. 103–107. [CrossRef]

22. Ismael, S.M.; Aleem, S.H.A.; Abdelaziz, A.Y.; Zobaa, A.F. Practical considerations for optimal conductor reinforcement and hosting capacity enhancement in radial distribution systems. *IEEE Access* **2018**, *6*, 27268–27277. [CrossRef]

23. Kumari, M.; Singh, V.; Ranjan, R. Optimal selection of conductor in RDS considering weather condition. In Proceedings of the 2018 International Conference on Computing, Power and Communication Technologies (GUCON), Greater Noida, India, 28–29 September 2018; pp. 647–651. [CrossRef]

24. Ismael, S.M.; Aleem, S.; Abdelaziz, A.Y. Optimal conductor selection in radial distribution systems using whale optimization algorithm. *J. Eng. Sci. Technol.* **2019**, *14*, 87–107.

25. Ramana, T.; Nararaju, K.; Ganesh, V.; Sivanagaraju, S. Customer Loss Allocation Reduction Using Optimal Conductor Selection in Electrical Distribution System. In *Emerging Trends in Electrical, Communications, and Information Technologies*; Springer: Berlin/Heildeberg, Germany, 2020; pp. 369–379. [CrossRef]

26. Martínez-Gil, J.F.; Moyano-García, N.A.; Montoya, O.D.; Alarcon-Villamil, J.A. Optimal Selection of Conductors in Three-Phase Distribution Networks Using a Discrete Version of the Vortex Search Algorithm. *Computation* **2021**, *9*, 80. [CrossRef]

27. Thenepalle, M. A comparative study on optimal conductor selection for radial distribution network using conventional and genetic algorithm approach. *Int. J. Comput. Appl.* **2011**, *17*, 6–13. [CrossRef]

28. Samal, P.; Mohanty, S.; Ganguly, S. Simultaneous capacitor allocation and conductor sizing in unbalanced radial distribution systems using differential evolution algorithm. In Proceedings of the 2016 National Power Systems Conference (NPSC), Bhubaneswar, India, 19–21 December 2016; pp. 1–6. [CrossRef]

29. Abul'Wafa, A.R. Multi-conductor feeder design for radial distribution networks. *Electr. Power Syst. Res.* **2016**, *140*, 184–192. [CrossRef]

30. Nivia Torres, D.J.; Salazar Alarcón, G.A.; Montoya, O.D. Selección óptima de conductores en redes de distribución trifásicas utilizando el algoritmo metaheurístico de Newton. *Ingeniería* **2022**, *27*, e19303. [CrossRef]

31. Montoya, O.D. Notes on the Dimension of the Solution Space in Typical Electrical Engineering Optimization Problems. *Ingeniería* **2022**, *27*, e19310. [CrossRef]

32. Zhang, Y.; Jin, Z.; Mirjalili, S. Generalized normal distribution optimization and its applications in parameter extraction of photovoltaic models. *Energy Convers. Manag.* **2020**, *224*, 113301. [CrossRef]

33. Cortés-Caicedo, B.; Avellaneda-Gómez, L.S.; Montoya, O.D.; Alvarado-Barrios, L.; Chamorro, H.R. Application of the Vortex Search Algorithm to the Phase-Balancing Problem in Distribution Systems. *Energies* **2021**, *14*, 1282. [CrossRef]

34. Abdel-Basset, M.; Mohamed, R.; Abouhawwash, M.; Chang, V.; Askar, S. A local search-based generalized normal distribution algorithm for permutation flow shop scheduling. *Appl. Sci.* **2021**, *11*, 4837. [CrossRef]

35. Wang, C.; Liu, P.; Zhang, T.; Sun, J. The adaptive vortex search algorithm of optimal path planning for forest fire rescue UAV. In Proceedings of the 2018 IEEE 3rd Advanced Information Technology, Electronic and Automation Control Conference (IAEAC), Chongqing, China, 12–14 October 2018; pp. 400–403. [CrossRef]

36. Doğan, B. A modified vortex search algorithm for numerical function optimization. *arXiv* **2016**, arXiv:1606.02710. [CrossRef]